Haverford College

Haverford Scholarship

Faculty Publications

Astronomy

1987

6 centimeter radio-source counts and spectral index studies down to 0.1 millijansky

Bruce Partridge
Haverford College, bpartrid@haverford.edu

R. Hank Donnelly '86
Class of 1986, Haverford College

R. A. Windhorst

Follow this and additional works at: https://scholarship.haverford.edu/astronomy_facpubs

1987

6 centimeter radio-source counts and spectral index studies down to 0.1 millijansky

Bruce Partridge
Haverford College, bpartrid@haverford.edu

R. Hank Donnelly '86
Class of 1986, Haverford College

R. A. Windhorst

Repository Citation

1987

6 centimeter radio-source counts and spectral index studies down to 0.1 millijansky

R. Bruce Partridge
Haverford College

R. Hank Donnelly '86
Class of 1986, Haverford College

R. A. Windhorst

Follow this and additional works at: http://scholarship.haverford.edu/astronomy_facpubs

6 CENTIMETER RADIO SOURCE COUNTS AND SPECTRAL INDEX STUDIES DOWN TO 0.1 MILLIJANSKY

R. Hank Donnelly and R. Bruce Partridge
Astronomy Department, Haverford College

AND

Rogier A. Windhorst
Mount Wilson and Las Campanas Observatories, Carnegie Institution of Washington

ABSTRACT

We present the results of a deep VLA survey at 6 cm in the Lynx.2 area of the Leiden Berkeley Deep Survey. This area was surveyed previously with the VLA at 21 cm as reported by Windhorst et al. in 1985. The survey sensitivities are ~15 and 28 μJy, at 6 and 21 cm, respectively. In our three 6 cm fields, chosen within the 21 cm survey area, 58 radio sources were found. Of these, 30 form a complete sample above the 5 σ level in 4.86 GHz flux density and within 7' of the center of one of the fields. For another 22 radio sources detected in the original 1.46 GHz survey, upper limits are given to the 4.86 GHz flux.

The slope of the normalized differential source counts at 6 cm is $\gamma \approx 1.8$ ($dN/dS \propto S^{-\gamma}$). The data from this and other 6 cm source counts are consistent with the flattening of the differential source counts found previously at 21 cm below a few mJy, although the change in slope cannot be derived from the 6 cm counts alone, due to the limited statistics.

Deep optical identifications and photometry of these sources are derived from the work of Kron, Koo, and Windhorst published in 1985. They are based on four-band ($UJFN$) Kitt peak 4 m plates. Available spectroscopic redshifts are also listed.

In a complete sample of 54 radio sources defined at 1.46 GHz, 26 (48%) are reliably identified down to the 4 m plate limits ($V \lesssim 23.2$ mag). Two identifications are Galactic stars, about a quarter are quasars, and the remainder are red giant elliptical galaxies and blue galaxies. The fraction of blue galaxies increases towards fainter radio fluxes, consistent with previous work. The redshifts of the blue radio galaxies, which we believe are largely responsible for the change in slope of the 21 cm source counts, are in the range $0.05 \lesssim z \lesssim 0.5$ for galaxies with $V < 22$ mag. Hence, the change in the slope of the source counts does not appear to be caused by a local population of dwarf galaxies at very low redshifts, but is most likely caused by a blue radio galaxy population at intermediate redshifts.

The 4.86–1.46 GHz spectral index distributions are presented for both the complete 6 cm and the complete 21 cm samples in two flux intervals. The median spectral index remains about 0.75, even down to $S_{1.46} \approx 0.25$ mJy. Although the fraction of flat spectrum sources ($\alpha < 0.5$) increases from 22% at $S_{1.46} \gtrsim 0.5$ to 41% at $0.25 \leq S_{1.46} < 0.5$ mJy, the majority of the sub-mJy 21 cm sources are of the steep spectrum class. The blue radio galaxies generally have steep spectra and compact radio morphology. Radio sources with the steepest spectra ($\alpha > 1.0$) are mostly unidentified on the 4 m plates. Three point spectral indices are given for radio sources with $S_{1.46} > 0.9$ mJy. The radio sources unidentified on the 4 m plates have mostly convex or concave spectra. We argue that they are most likely high-redshift red or blue galaxies, respectively.

Subject headings: cosmology — quasars — radio sources: galaxies — radio sources: identifications — radio sources: spectra

I. INTRODUCTION

Recently a 21 cm survey made down to millijansky levels with the Westerbork Synthesis Radio Telescope with a total area of 5.5 deg^2 (Windhorst, van Heerde, and Katgert 1984, hereafter WHK). This Leiden-Berkeley Deep Survey (or LBDS) had one area of 0.67 deg^2 without 21 cm radio sources stronger than 5 mJy. This particular field, Lynx.2, was followed up by a deep VLA[1] 21 cm survey with a 1 σ map noise of 28 μJy (by Windhorst et al. 1985, hereafter WMOKK).

In these surveys the differential source counts were computed normalized to the expected counts in a homogeneous, static, Euclidean universe. The normalized differential source counts in the Lynx.2 field showed a significant change in their slope below 5 mJy (see also Windhorst 1984, hereafter W84). This "upturn," or rather flattening of the counts, was confirmed by an independent deep 21 cm Westerbork survey of the same area by Oort and Windhorst (1985, hereafter OW), and it also appears to be present in a deep VLA 21 cm survey of another area by Condon and Mitchell (1984). In addition, it was suggested in deep 6 cm VLA surveys of different areas—albeit with limited statistics—by Fomalont et al. (1984) and by Partridge, Hilldrup, and Ratner (1986, hereafter PHR). Hence the change in slope, or "upturn" in the millijansky counts is not due to instrumental effects, but is a property of the universe.

This upturn in the counts is significant because it cannot

easily be attributed to any one of the canonical radio source populations. It cannot be due to the epoch-dependent radio luminosity function (RLF) of giant elliptical radio galaxies and quasars, because these objects dominate the counts only for $S_{1.46} \gtrsim 5$ mJy; nor can it be explained by the RLF of normal spiral and Seyfert galaxies, unless these objects have undergone significant cosmological evolution in the recent past (see van der Laan et al. 1983). As a consequence, various models have been developed in the recent literature that incorporate other scenarios or radio source populations which contribute to the counts below 5 mJy. For instance, Condon (1984) explains the upturn in the 21 cm counts by evolving the RLF of normal spiral galaxies quite drastically with cosmic epoch, an effect which has not been confirmed by direct observations. Wall et al. (1986) and Subrahmanya (1968) explain the upturn by invoking a nonevolving population of low luminosity galaxies that dominate the local RLF at very low radio powers.

In order to help determine the nature of the radio sources that cause the upturn in the counts, optical identifications were made for the LBDS sample on four-band (UJFN) Kitt Peak 4 m plates down to $V \approx 23.2$ mag (Windhorst, Kron, and Koo 1984, hereafter WKK). Multicolor photometry is presented from the same plates by Kron, Koo, and Windhorst (1985, hereafter KKW), together with about 60 spectroscopic redshifts down to $V \approx 22.0$ mag. On the 4 m plates, 53% of the LBDS radio sources were reliably identified. About 80% of the mJy radio source identifications are red and blue radio galaxies. The remainder are quasars. The red galaxies are spectroscopically like "standard candle" giant ellipticals and are the dominant population at millijansky levels.

At the submillijansky level, about a quarter of the identifications are quasars and, in a few other cases, Galactic stars. The remaining sub-mJy identifications are red and blue radio galaxies, with an increasing fraction of blue radio galaxies at fainter radio fluxes (WMOKK). A minority of these blue radio galaxies are normal spiral galaxies at redshifts of 0.05–0.15, but the majority are faint blue galaxies at larger redshifts, sometimes with peculiar optical morphology, indicative of interacting or merging galaxies (KKW).

It is this population of blue radio galaxies that was held responsible by W84 and WMOKK for the upturn in the source counts. Although there is evidence to support this view, the nature of this blue radio galaxy population is still not very well known. W84 presented a model that invokes some RLF evolution for the blue radio galaxy population to reproduce the steep slope of the sub-mJy source counts. This, like other suggestions noted above, needs to be verified observationally. The most important question concerns the true nature of the blue sub-mJy radio galaxies. Is their radio emission nonthermal, either from a nonthermal nucleus or the integrated supernova emission in the disk, or is it of thermal origin instead? In order to answer these questions, one needs two-point and three-point

spectral indices and higher resolution maps. And, equally important, one needs to study carefully the optical identifications of the sub-mJy radio sources.

In this paper we will deal primarily with the two-point and three-point spectral indices. The purpose of this paper is twofold. First, we want to confirm the amplitude and slope of the 6 cm source counts found by Fomalont et al. (1984) and PHR at submillijansky levels by observing another, independent area. Second, we investigate the spectral index distributions of the sub-mJy population, as a function of both 6 and 21 cm flux density and of optical identification class.

Section II of this paper presents the radio observations and data reduction. Section III describes the available information on optical identifications, photometry and spectroscopy. Section IV presents the 6 cm source counts. In § V we present and analyze the spectral index distributions as a function of flux density and optical identification class. In § VI the results are discussed.

II. THE OBSERVATIONS

The observations were carried out with the Very Large Array in its D configuration on the nights of 1986 January 22, 23, and 26. Two frequency bands, centered at 4835 and 4885 MHz, each MHz wide, were used for the observations. At the central frequency of 4860 MHz ($\lambda \approx 6$ cm) the synthesized beam of the instrument has HPBW(R.A.) × HPBW(decl.) $\approx 17'' \times 16''$, comparable to the resolution achieved at 21 cm (WMOKK). A description of the VLA has been given by Thompson et al. (1980).

a) Field Centers

The centers of the three 6 cm fields we observed are given in Table 1. They were chosen in such a way that 60 of the 130 radio sources detected in the 21 cm map, and 54 of the 99 sources in the complete 21 cm sample of WMOKK, were within 9', of one of the 3 field centers. At 6 cm, 9' is approximately the primary beam radius to the first null of the VLA telescopes. The field centers were optimized to cover the maximum number of known 21 cm sources with the smaller 6 cm fields. This bias must be kept in mind when considering the 6 cm counts.

During our first night of observations, an instrumental problem effectively eliminated half our data. We choose to use the remaining nights to obtain equal integration time (~ 8 hr on each) on fields W1 and W2 and fewer observations of field W3, since it contained only 11 of the 21 cm sources.

b) Calibration and Editing of the Data

Our primary flux calibrator was 3C 286, for which we assumed a flux density of 7.46 Jy at 4835 MHz, and 7.41 Jy at 4885 MHz, bringing all fluxes on the scale of Baars et al. (1977). As secondary phase and flux calibrators we used 3C 48

TABLE 1

THE 6 CENTIMETER SURVEY FIELDS

FIELD NAME (1)	FIELD CENTER		RMS MAP NOISE (μJy) (4)	5 σ PEAK THRESHOLD (μJy) (5)	COMPLETENESS IN INTEGRATED FLUX (μJy) (6)	NUMBER OF 21 CENTIMETER SOURCES (7)
	R.A. (1950) (2)	Decl. (1950) (3)				
Wind 1.........	$8^h41^m11^s$	$+44°55'40''$	15.58	77.9	100	25
Wind 2.........	8 41 24	$+44\ 42\ 37$	15.28	76.4	98	24
Wind 3.........	8 42 57	$+44\ 40\ 33$	21.30	106.5	136	11

and 0833 + 585; our calibrations were done every 20 minutes and had an accuracy of 2% in amplitude, with phase errors $\lesssim 5°$.

Summaries of the visibility data were inspected for interference, noisy correlators, and phase jumps, and all suspect data were dropped. We found it necessary to eliminate only a few percent of the visibility records (after discarding the bad half of the first night's data).

c) 6 Centimeter Maps

Using the standard Fourier transform programs available at NRAO, we made maps of each of the three 6 cm fields surveyed. The image size was 1024 cells on a side, and we used 4" cells. The visibility data were given natural weight in the gridding process preceding the Fourier transform of the u-v data; that is, the weight assigned to the data at a given grid point in the u-v plane was proportional to the number of visibility data in that point. Then the inner 512^2 cells of the maps were CLEANed, using the standard NRAO program APCLN with a loop gain of 0.2. We cleaned 100 components in the fields W2 and W3, and 175 components in field W1 which had more discrete sources.

We measured the rms noise of the three maps in regions well away from discrete sources, where we expect instrumental noise to dominate. The results are shown in Table 1 and are within 10% of the rms values expected for instrumental noise alone. Note that the rms noise level of the field W3 is larger because we obtained only half as many observations of it.

d) Correction of the Maps for the Primary Beam Response

The maps referred to above were not corrected for the primary beam response of the VLA antennas. For each field, we also made a map to which we applied the correction for the primary beam response. In such maps, sources appear with their true flux density, but the instrumental noise is also multiplied up by the primary beam correction. The correction was applied to the inner 9' of each field, at which radius the primary beam response has fallen to ~3%. The boundary we employed in our source counts is $r \leq 7'$, where the primary beam response is well known and $\geq 16.8\%$ (−7.8 dB).

e) Source Definition

We first visually inspected the VLA maps of the three 6 cm fields, noting the position of apparent sources. We then fixed a threshold of 4 times the rms noise in each 6 cm map and located all sources with peak fluxes exceeding the corresponding 4 σ threshold. In total 58 sources were found in the three 6 cm fields.

f) Determination of Fluxes

Once candidate sources had been located in the maps, we determined fluxes for them by fitting two-dimensional Gaussian profiles to their surface brightness distribution. The fitted parameters were half-widths along the major and minor axis, right ascension, declination, position angle, peak flux, and integrated flux density. Two independent fits for each source were made with different starting values. We made model fits to sources in both the uncorrected maps and the maps that were corrected for primary beam response. In the former case, we multiplied the integrated model flux densities by the appropriate value of the primary beam correction as derived from Napier and Rots (1982). With a single exception (source 4 in

field W1), the various determinations of flux density agreed within their errors.

We also made two-dimensional Gaussian fits to potential sources located within 10" of the positions of 21 cm sources even when these sources had peak fluxes below the 4 σ threshold in our 6 cm maps. The resulting values for the integrated flux density were used in § V to determine limits to the spectral indices of these sources.

g) The 6 Centimeter Source Catalog

The *complete* 6 cm sample was restricted to the inner 7' of each field, where the primary beam response is $\geq 16.8\%$. As for the complete 21 cm sample of WMOKK, we further required that the peak flux density of each candidate source be greater than or equal to 5 times the noise of the corresponding map.

To establish the completeness limit of our 6 cm sample in terms of integrated flux, we need to take into account the fact that the integrated flux density of resolved and extended sources is usually larger than their peak intensity. In the present work, we find the mean ratio of the integrated to peak flux density for sources to be 1.16 ± 0.06, in excellent agreement with the values found by Fomalont et al. (1984) and PHR. To be conservative, we take as the completeness limit for each field 1.28 times the corresponding 5 σ threshold on peak flux for that field; that is, we are confident at about the 2 σ level that we have not missed sources below this limit because their peak flux fell below our 5 σ threshold. This procedure is justified, because the angular size distribution of radio sources at the mJy level is very narrow (OW; Coleman and Condon 1985; Oort et al. 1987). Also, bandwidth smearing does not reduce S_p by more than 5%, even at 7' from the map center. The resulting completeness limits are listed in column 6 of Table 1 and are the ones used to define the complete 6 cm source sample with Table 2. Only one source was excluded from the sample by these requirements, leaving us with a total of 30 sources in our complete 6 cm sample that can be used for the source counts.

h) Coincidences with 21 Centimeter Sources

When a source in one of our 6 cm maps lay within 10" in both R.A. and decl. from a 21 cm source in the catalog of WMOKK, we accepted it as a real coincidence. Thus a 6 cm source was considered to be the counterpart of a 21 cm source only if its difference in position was significantly less than one beam area. This is a necessary requirement in order not to miss 21-6 cm coincidences of low surface brightness sources. Except for a few very low surface brightness sources, the 21-6 cm positional correspondence was usually better than 4". Even for sources at the edge of our maps, where uncertainties in the effective frequency of the IF bands might cause position shifts, the 6 cm positions were within 1–3" from the 21 cm positions and those of the optical identifications.

Among the sources listed in the original 21 source catalog of WMOKK as double, there were five for which we now have good reasons to believe are unrelated, individual point sources, and we so show them in Table 2 here. Because the angular size distribution at ~1 mJy recently has been found to be narrower than previously thought (OW; Coleman and Condon 1985; Oort et al. 1987), the criterion used by WHK that two nearby point sources are to be considered as one physical double if they are closer than 50" no longer is appropriate for sources with $S_{1.46} \lesssim 1$ mJy. Consequently, the 21 cm sources 60A and 60B, as well as 70A, 70B, and 70C, would have unrealistically

TABLE 2

THE SOURCE CATALOG

Source number 6cm/fld	21cm	RA(1950)	DEC(1950)	S1462 (error) (mJy)	S4860 (error) (mJy)	alpha (error)		ID	U-mag	J-mag	F-mag	N-mag	z	LR	FL
1/W1*	25*	8 40 40.0	45 00 29.3	0.59 (0.15)	0.59 (0.18)	0.00 (0.33)	F	BG?	22.89	23.00	22.19	20.93		22.99	2
--*	24	8 40 40.2	44 42 11.2	1.24 (0.11)	<0.48 (0.16)	>0.78 (0.28)	S	Q	22.30	22.66	22.99	>21.1		199.52	0
2/W1*	26	8 40 42.7	44 52 32.8	0.81 (0.13)	0.28 (0.07)	0.88 (0.24)	S	-						0.00	1
3/W1	28	8 40 43.8	44 55 11.8	0.61 (0.10)	0.38 (0.05)	0.39 (0.17)	F	RG	>23.5	23.68	21.69	19.57		23.02	0
4/W1	29	8 40 45.2	44 58 30.5	0.51 (0.08)	0.72 (0.08)	-0.29 (0.17)	I	Q	22.05	23.10	22.47	>21.1		9.08	0
--*	31	8 40 48.6	44 42 6.7	0.44 (0.06)	<0.19 (0.06)	>0.71 (0.29)	S	BG	22.04	22.28	20.59	19.52		27.80	1
5/W2	32	8 40 50.8	44 45 52	1.65 (0.10)	1.12 (0.13)	0.32 (0.11)	F	-						0.00	0
6/W1	33	8 40 51.0	44 49 45.1	4.64 (0.23)	4.50 (0.10)	0.03 (0.05)	F	Q	21.74	21.21	21.17	21.33		225.41	0
7/W2	35	8 40 53.5	44 46 29	0.42 (0.06)	0.61 (0.04)	-0.31 (0.13)	S	RG?	23.50	>23.7	21.85	20.19		>2.0	0
--*	36	8 40 53.8	44 45 11	0.41 (0.08)	0.34 (0.09)*	-0.16 (0.27)	F	B?	23.54	>23.7	>22.7	>21.1		2.04	0
8/W1*	--*	8 40 56.2	44 58 45.4	<0.17 (0.06)	0.11 (0.04)	0.36 (0.42)	F								
9/W1*	39	8 40 57.2	44 50 40.8	0.28 (0.05)	0.22 (0.08)	0.20 (0.33)	F	S	16.20	16.10	15.68	14.29	0.000	2.31	0
10/W2*	--*	8 40 57.4	44 39 26	<0.13 (0.04)	0.25 (0.08)	<-0.54 (0.37)	I	-						0.00	1
11/W2*	40	8 40 58.1	44 45 18	0.93 (0.17)	0.60 (0.06)	0.36 (0.17)	F	-						0.00	1
12/W1*	42	8 41 0.5	44 54 24.7	0.27 (0.06)	0.19 (0.03)	0.29 (0.22)	F							18.58	2
13/W1	43*	8 41 2.3	44 56 24.5	0.24 (0.06)	0.10 (0.02)	0.73 (0.26)	S	BG	20.74	20.35	19.46	18.47		45.06	0
14/W1	44	8 41 3.5	44 54 0.8	1.91 (0.12)	0.54 (0.02)	1.05 (0.06)	S	S	15.89	16.02	15.64	13.82	0.000	17.52	2
15/W1*	45*	8 41 3.5	44 59 12.1	0.40 (0.10)	0.07 (0.05)	1.45 (0.62)	S	BG	19.64	19.58	18.65	17.74		0.00	1
16/W2	46	8 41 6.0	44 42 59	0.33 (0.05)	0.29 (0.02)	0.11 (0.14)	F	-						0.00	
17/W1*	--*	8 41 7.5	45 02 12.7	<0.20 (0.06)	<0.65 (0.02)	<-0.97 (0.30)	S	-						0.00	1
--*	47	8 41 8.6	44 54 47	0.29 (0.06)	0.64 (0.02)	>1.50 (0.39)	S	RG	22.88	22.11	20.03	18.73		51.82	2
18/W2	49*	8 41 8.6	44 40 38	0.26 (0.06)	0.72 (0.03)	-0.85 (0.19)	I	-						0.00	1
19/W1	48	8 41 8.7	45 01 09.2	2.71 (0.20)	1.15 (0.04)	0.71 (0.07)	S	-						0.00	1
20/W1	50	8 41 9.7	44 57 3.9	0.43 (0.08)	0.29 (0.06)	0.32 (0.23)	F	-						8.44	0
21/W1	51	8 41 10.9	44 59 53	0.48 (0.09)	0.72 (0.03)	0.42 (0.18)	S	BG?	22.53	22.92	21.53	>21.1		96.32	0
22/W1	52	8 41 11.0	44 56 56.0	1.35 (0.12)	0.72 (0.08)	0.52 (0.08)	S	R?	>23.5	>23.7	>22.7	21.53		0.00	1
23/W2	54	8 41 13.0	44 42 32	0.38 (0.06)	0.17 (0.03)	0.67 (0.19)	S	-						0.00	1
24/W1	53	8 41 13.4	45 01 29	0.74 (0.10)	0.31 (0.04)	0.72 (0.15)	S	-						0.00	1
25/W1	--*	8 41 13.8	44 52 11.0	0.16 (0.04)*	0.21 (0.02)	-0.23 (0.21)	I	-						0.00	1
26/W2*	55A	8 41 13.8	44 36 52	2.36 (0.14)	0.26 (0.07)	1.04 (0.22)	S	-						0.00	0
--*	55B	8 41 16.0	44 36 32	0.37 (0.07)	0.18 (0.06)	0.59 (0.32)	S	-						9.61	0
27/W1	57	8 41 18.5	44 56 26.5	0.80 (0.10)	0.21 (0.03)	>1.11 (0.16)	S	BG	18.24	18.14	17.14	16.34	0.147	5.53	1
28/W1*	58	8 41 19.6	44 58 13.7	0.27 (0.05)	0.09 (0.04)	0.91 (0.40)	S	RG?	>23.5	23.66	21.73	20.30		0.00	1
29/W1*	60A	8 41 19.6	44 54 48.0	0.40 (0.08)	0.06 (0.03)	1.58 (0.44)	S	-						0.00	1
--*	59	8 41 20.0	44 59 9.6	0.25 (0.05)	0.08 (0.03)	1.00 (0.37)	S	-						0.00	1
30/W2	61	8 41 21.4	44 43 19	0.92 (0.06)	0.37 (0.02)	>0.76 (0.07)	S	-						0.00	1
31/W1*	60B	8 41 22.5	44 54 42.7	0.35 (0.06)	0.08 (0.02)	1.23 (0.25)	S	BG	22.36	23.12	22.19	20.85		17.72	1
--*	62*	8 41 22.7	44 39 52.8	0.31 (0.07)	0.06 (0.02)	>1.39 (0.34)	S	BG	18.82	18.70	17.80	17.00	0.16	171.61	2
32/W1	63	8 41 22.9	44 55 32.3	1.61 (0.09)	0.64 (0.02)	0.77 (0.05)	S	-						0.00	0
33/W1*	--*	8 41 23.0	44 57 25.7	<0.12 (0.04)	0.17 (0.04)	-0.29 (0.34)	S	B?	23.78	22.96	22.36	22.03		81.93	2
--*	64*	8 41 26.8	44 46 47.3	0.18 (0.03)	0.08 (0.03)	>-0.66 (0.36)	S	-						0.00	1
34/W2*	--*	8 41 27.5	44 40 22	<0.10 (0.03)	0.15 (0.02)	<-0.34 (0.27)	I	-						0.00	0
35/W1	65	8 41 30.4	44 57 16.4	1.75 (0.10)	0.74 (0.04)	0.72 (0.06)	S	-						93.23	1
36/W1*	66	8 41 31.7	44 52 34.7	0.35 (0.05)	0.19 (0.06)	0.53 (0.29)	S	Q	22.45	22.47	22.17	>21.1		0.00	0
--*	67	8 41 32.3	44 47 50.5	0.25 (0.04)	<0.13 (0.04)	>0.57 (0.30)	S	-						33.25	1
--*	68*	8 41 33.0	44 45 43.3	0.19 (0.05)	0.07 (0.02)	>0.86 (0.33)	S	Q	18.37	18.41	18.40	17.84		0.00	2
--*	69A	8 41 37.7	44 39 22.8	0.36 (0.07)	0.08 (0.03)*	>1.27 (0.36)	S	-						0.00	1

(1)	(2)	(3) R.A. (1950)	(4) Decl. (1950)	(5) S_{21}	(6) S_6	(7) α	(8)	(9)	(10) U	(11) J	(12) F	(13) N	(14) z	(15) LR	(16) FL
--- *	57	8 41 20.0	44 43 19	7.0	0.25 (0.05)	0.05 (0.05)	>1.00 (0.37)	S	--						0.00	1
30/W2	61	8 41 21.4	44 54 42.7	19	0.92 (0.06)	0.37 (0.02)	0.76 (0.07)	S	--						0.00	1
31/W1*	60B	8 41 22.5	44 54 42.7	42.7	0.35 (0.06)	0.08 (0.02)	1.23 (0.25)	S	BG	22.36	23.12	22.19	20.85		0.00	1
--- *	62*	8 41 22.7	44 39 52.8	52.8	0.31 (0.07)	0.06 (0.02)	<0.39 (0.34)	S	BG	18.02	18.70	17.00	17.00	0.16	17.72	2
32/W1	63	8 41 22.9	44 55 32.3	32.3	1.61 (0.09)	0.64 (0.02)	1.39 (0.05)	S	BG						171.61	0
33/W1*	--- *	8 41 23.0	44 57 25.7	25.7	<0.12 (0.04)	0.17 (0.04)	0.77 (0.34)	I	--							
--- *	64*	8 41 26.0	44 46 47.3	47.3	0.18 (0.04)	0.08 (0.03)	<0.29 (0.34)	I	B?	23.78	22.96	22.36	22.03		81.93	2
34/W2*	--- *	8 41 27.5	44 40 22	22	<0.10 (0.03)	0.15 (0.02)	0.66 (0.36)	S	--							
--- *	65	8 41 30.4	44 57 16.4	16.4	1.75 (0.10)	0.74 (0.04)	<0.34 (0.27)	I	--						0.00	1
35/W1	66	8 41 31.7	44 52 34.7	34.7	0.35 (0.05)	0.19 (0.06)	0.72 (0.06)	S	Q	22.45	22.47	22.17	>21.1		93.23	0
36/W1*	67	8 41 32.3	44 47 50.5	50.5	0.25 (0.04)	0.13 (0.04)	0.53 (0.29)	S	--						0.00	1
--- *	68*	8 41 33.0	44 45 43.3	43.3	0.19 (0.05)	0.07 (0.02)	0.57 (0.30)	S	Q	18.37	18.41	18.40	17.84	33.25		2
--- *	69A	8 41 37.7	44 39 22.8	22.8	0.36 (0.07)	0.08 (0.03)*	0.86 (0.33)	S	Q						0.00	1
37/W1*	--- *	8 41 38.0	44 56 43.6	43.6	<0.11 (0.04)	0.13 (0.04)	1.27 (0.36)	I	--							
38/W1*	--- *	8 41 39.3	44 58 48.7	48.7	<0.13 (0.04)	0.27 (0.05)	<0.14 (0.40)	F	--							
--- *	69B	8 41 39.3	44 39 10	10	1.06 (0.09)	0.79 (0.05)	<0.61 (0.36)	S	--						0.00	1
39/W2	71	8 41 41.2	44 55 5	5	0.48 (0.06)	0.19 (0.05)	0.24 (0.09)	S	--						0.00	1
40/W1*	--- *	8 41 41.4	44 52 1.8		0.27 (0.05)	0.21 (0.07)	0.79 (0.24)	F	BG?	23.50	22.79	21.30	20.41		8.58	0
--- *	70C	8 41 41.5	44 52 26.4	26.4	0.35 (0.07)	0.27 (0.11)	0.21 (0.32)	F	--						0.00	1
41/W1	70A	8 41 42.2	44 51 38.7	38.7	0.37 (0.06)	0.63 (0.12)	0.22 (0.37)	F	--						0.00	1
42/W1	70B	8 41 42.2	44 36 40	40	2.85 (0.16)	0.75 (0.11)	-0.44 (0.21)	I	--						0.00	1
--- *	72	8 41 42.4	44 46 13.7	13.7	0.20 (0.04)	0.10 (0.03)	1.11 (0.13)	S	BG	17.22	16.26	15.31	13.42		59.31	2
43/W2*	73*	8 41 42.9	44 37 11.9	11.9	0.32 (0.06)	0.19 (0.06)	0.56 (0.30)	S	BG	22.21	22.15	20.88	19.55		111.41	0
--- *	74	8 41 44.8	44 45 34.0	34.0	0.18 (0.03)	0.10 (0.03)	0.42 (0.30)	F	RG	23.08	23.14	21.21	20.62		79.39	2
--- *	75*	8 41 50.7	44 45 41.5	41.5	0.22 (0.05)	0.14 (0.05)	0.52 (0.29)	S	BG	21.01	21.73	20.52	19.62		0.53	2
--- *	77*	8 41 55.6	44 46 40.0	40.0	0.36 (0.04)	0.26 (0.05)	0.39 (0.36)	F	BG	21.74	21.31	19.86	18.69	0.425	141.05	0
--- *	80	8 41 57.0	44 42 8.0	8.0	0.15 (0.03)	0.16 (0.05)	<0.27 (0.30)	I	BG	17.22	16.22	15.19	13.20	0.05	25.39	2
--- *	82*	8 42 4.9	44 43 35.6	35.6	0.53 (0.06)	0.34 (0.11)	-0.07 (0.30)	F	--						0.00	1
--- *	85	8 42 23.6	44 36 10.0	10.0	1.93 (0.13)	0.49 (0.16)	0.37 (0.29)	S	--						0.00	1
--- *	94	8 42 30.0	44 37 38	38	0.48 (0.09)	0.58 (0.04)	1.14 (0.28)	I	RG	>23.5	22.96	20.97	19.40		6.68	0
--- *	97	8 42 30.1	44 36 50	50	<0.15 (0.05)	0.18 (0.10)	-0.16 (0.16)	I	--							
44/W3	--- *	8 42 38.8	44 46 48.9	48.9	0.46 (0.07)	0.39 (0.13)	-0.15 (0.54)	F	Q?	22.41	23.32	22.59	21.38		4.18	0
45/W3*	98	8 42 39.3	44 40 7	7	0.60 (0.11)	0.06 (0.05)	0.13 (0.30)	S	BG	22.06	22.34	20.90	19.79		2.56	0
--- *	99	8 42 41.3	44 41 52	52	0.38 (0.06)	0.14 (0.05)	1.92 (0.70)	S	BG	20.80	21.50	20.35	19.60		8.13	0
46/W3*	101	8 42 44.9	44 47 46.2	46.2	0.95 (0.08)	0.54 (0.18)	0.83 (0.32)	F	RG?	22.95	>23.7	22.08	20.71		72.05	0
47/W3	104	8 42 52.0	44 43 3	3	<0.13 (0.04)	0.11 (0.09)	0.46 (0.28)	F	--							
--- *	105A	8 43 00.2	44 41 14	14	1.96 (0.24)	0.67 (0.09)	0.14 (0.40)	S	Q	21.53	21.76	21.36	21.42	1.10	~2.0	2
48/W3*	105B	8 43 04.0	44 40 57	57	1.79 (0.17)	0.68 (0.05)	0.89 (0.15)	S	RG	22.85	21.86	20.05	18.73	0.402	4.31	0
49/W3	--- *	8 43 06.4	44 40 36	36	<0.17 (0.06)	0.36 (0.04)	0.81 (0.10)	I	--							
50/W3	--- *	8 43 09.2	44 44 15	15	<0.17 (0.06)	0.16 (0.05)	<0.61 (0.31)	F	--							
51/W3	--- *	8 43 12.5	44 44 13	13	0.33 (0.07)*	0.34 (0.03)	0.05 (0.39)	I	--							
52/W3*	108	8 43 12.7	44 41 54	54	2.31 (0.17)	0.73 (0.04)	-0.02 (0.20)	S	RG	23.33	>23.7	21.96	20.11	0.72	208.92	0
53/W3	--- *	8 43 14.5	44 44 35.5	35.5	<0.18 (0.06)	0.37 (0.10)	0.96 (0.08)	I	--							
54/W3	111	8 43 16.4	44 44 38	38	0.67 (0.12)	0.36 (0.11)	<0.60 (0.36)	S	BG	19.20	18.02	17.69	16.54	0.125	26.94	0
55/W3*	--- *	8 43 23.5	44 47 43	43	<0.22 (0.07)	1.68 (0.77)	0.52 (0.29)	I	--							
56/W3*	--- *	8 43 35.4	44 33 33	33	2.05 (0.26)	0.59 (0.30)	<-1.67 (0.47)	I	--							
57/W3*	113						1.31 (0.42)	S	--						0.00	1

COL. (1).—6 cm source number and 6 cm field where the source was found (asterisk means source not in complete 6 cm sample).
COL. (2).—21 cm source number (asterisk means source not in complete 21 cm sample).
COL. (3).—Right ascension of the 6 cm source for the equinox 1950. If not detected at 6 cm, then the 21 cm position is listed.
COL. (4).—Declination of the 6 cm source for the equinox 1950. If not detected at 6 cm, then the 21 cm position is listed.
COL. (5).—21 cm total sky flux and its error, or 3 σ upper limit. (Asterisk means source detected at <4 σ level in 21 cm map).
COL. (6).—6 cm total sky flux and its error, or 3 σ upper limit. (Asterisk means source detected at <4 σ level in 6 cm map).
COL. (7).—21–6 cm spectral index and its error. If source not detected at 21 or 6 cm, then an upper or lower limit is given.
COL. (8).—Spectral classification: S = steep (α > 0.5), F = flat (0 < α < 0.5), I = inverted (α < 0).
COL. (9).—Optical candidate: RG = red galaxy (gE), BG = blue galaxy (G?) = probable galaxy, ? = unknown object, Q = quasar, S = Galactic star.
COL. (10).—Photographic U magnitude.
COL. (11).—Photographic J magnitude.
COL. (12).—Photographic F magnitude.
COL. (13).—Photographic N magnitude.
COL. (14).—Spectroscopic redshift.
COL. (15).—Likelihood ratio LR. If LR > 2, then optical candidate is a likely identification.
COL. (16).—Flag: FL = 0 for reliable optical identifications in complete 21 cm sample; FL = 1 if no likely identification in the complete 21 cm sample; FL = 2 if possible optical identification, but radio source not in the complete 21 cm sample.

large angular sizes if they were treated as one double or triple source, and we now believe that they are all unrelated sources. The 21 cm sources 55A and 55B, and 69A and 69B, also are no longer considered to constitute physical double sources, because the flux ratios of their components would be too extreme given the distribution of WHK. The complex 21 cm source 105A and 105B probably also consists of two unrelated sources, because both sources have likely optical identifications confirmed by recent spectroscopy (see § III).

Once these corrections to the WMOKK catalog have been taken into account, we find that 39 of the 6 cm sources are coincident with cataloged 21 cm sources. The source names, equinox 1950 positions, 21 and 6 cm flux densities, spectral indices, and optical identifications are given in Table 2, which contains the following categories of sources:

1. All sources in our complete 6 cm sample, that is, those detected above the 5 σ threshold in S_p and within the 7' of one of the 6 cm field centers. Most of these corresponded with sources in the complete 21 cm sample of WMOKK, but 3 of the faintest 6 cm sources were not detected at 21 cm.

2. All other sources detected in our 6 cm maps that do not belong to the complete 6 cm sample (either $S_p < 5 \sigma$ or radius $> 7'$). These sources are marked with an asterisk behind their 6 cm name in the first column. Several of these were used to compute spectral indices for the fainter sources in the complete 21 cm sample.

3. All sources detected in the 21 cm of WMOKK that lie within our 6 cm fields. Those sources with an asterisk behind their 21 cm name in the second column do not belong to the complete 21 cm sample (either peak flux $S_p < 5 \sigma$ or primary beam radius > 25'.7 [attenuation < −10 dB]). Several of these were not detected at 6 cm.

A complete 6 cm sample can thus be derived from Table 2 by taking all sources without asterisks behind their 6 cm name in first column, while a complete 21 cm sample can be derived by taking all sources behind their 21 cm name in the second column.

III. OPTICAL IDENTIFICATIONS, PHOTOMETRY, AND REDSHIFTS

The optical identifications and the photometry are based on prime focus plates made with the Mayall 4 m telescope at Kitt Peak National Observatory. The plates were made in the photographic *UJFN* color system and have the following emulsion plus filter combinations (plus exposure times and limiting magnitudes for stellar objects): U: IIIa-J + UG5 (23.5 mag in 150 minutes); J: IIIa-J + GG385 (23.7 mag in 45 minutes); F: 127-02 + GG495 (22.7 mag in 65 minutes); N: IV-N + RG695 (21.2 mag in 60 minutes). The original 4 m plates were no longer available to us at the time the 6 cm survey was done. Hence no identification attempts were made for the new 6 cm sources that were not previously detected at 21 cm by WMOKK. For studies involving correlations with optical data one should thus use the sample selected at 21 cm.

a) The Optical Identification Procedure

The optical identifications are taken from WMOKK, and the identification procedure was described in detail by WKK, who also give a finding chart for the Lynx.2 field. The astrometry had systematic errors less than 0".2–0".3 in position, while the random errors are about 0".4. The overall error in the astrometry is about 0".5. The positional accuracy of the present 6 cm survey is about 1", comparable to the median positional error of 1".0 at 21 cm. The 21 cm positions are in fact slightly better than the 6 cm positions, because of the somewhat nar-

rower beam in the 21 cm maps (usually 14".7, but sometimes 11".3 in the high-resolution map of WMOKK) and the higher signal-to-noise ratio at 21 cm (for steep spectrum sources). Hence we use the actual 21 cm positions to compute the likelihood for individual identifications (calculations based on the 6 cm positions yielded similar results).

The candidate optical identifications are not farther away from the radio source position than 2.8 times the combined radio-optical error circle. For every radio source and optical candidate, the likelihood ratio (LR) was computed (using the procedure of WKK). The LR compares the probability that an optical object, once found at a certain radius from the radio source position, is the correct identification with the probability that it is a contaminating object. We define our complete sample of optical identifications as those candidates visible on the 4 m plates in at least one passband with LR ≥ 2.0 (i.e., the probability that the candidate is the correct identification is at least 2 times the probability that it is a spurious object).

The optical identification type (red or blue galaxy, quasar, or star) is listed in the ninth column of Table 2 and the likelihood ratios in the fifteenth column. In the sixteenth column we note whether an optical identification belongs to the radio-optical complete sample (see notes to Table 2).

b) Reliability of the Optical Identifications

The optical candidates indicated by the 6 cm positions were essentially always the same as those found from the 21 cm positions, because the 21 and 6 cm positions agreed in general to within 4", with the exception of a few low surface brightness sources. There are five identifications with a LR just in excess of 2.0, resulting in possibly doubtful identifications. For some of these, the new 6 cm position actually helped to establish the identification:

1. Radio source 35 from the 21 cm catalog is 3" north of a very red, faint object, presumably a galaxy. The resulting formal likelihood ratio is less than 2.0. However, the source has low surface brightness, and its 6 cm position (7/W2) is within 1" of the red object, which we therefore consider to be the correct identification.

2. 21 cm radio source 36 (marginally detected at 6 cm) is centered 4" west of a very faint, possibly low surface brightness, blue object, which was detected only on the U plate. Because the radio source also has low surface brightness on a deep contour plot of the 21 cm VLA map, with a position angle roughly east-west, it is possible that the faint blue object is the correct identification, since it is displaced along the east-west radio axis.

3. Radio source 9/W1 coincides with a bright, spectroscopically confirmed, star. Both at 21 and 6 cm the radio-optical position correspondence is fair (≤2".8). The other radio star in our sample, 14/W1, as well as the other LBDS radio stars (WKK, OW) usually show significant variability on time scales of a month to a year and, as a result, often appear to have very flat or steep spectral indices, because the observations at different frequencies were done at different epochs. The radio source 9/W1 was not detected at the 3.5 σ level in the 21 cm Westerbork map of OW, from which we derive a 3 σ upper limit $S_{1.46}(1982.0) \le 0.25$ mJy. Since the 21 cm VLA flux is 0.28 ± 0.05 mJy (also epoch 1982.0), we cannot make any claim for variability on the basis of the 21 cm observations alone. However, 9/W1 has a rather flat spectral index ($\alpha = 0.20$), which might be due to the actual presence of variability. We therefore suggest that the bright star is the correct identification.

4. Radio source 46/W3 is 4″ south of a faint blue galaxy. The radio source has low surface brightness at 21 cm and its 6 cm position is within 1″ of the blue galaxy, which we therefore consider to be the correct identification.

5. Radio source 49/W3 is associated with component A of 21 cm source 105, which was formerly believed to constitute a double source with 105B as the other component (see § IIe). Source 105B ($= 50/W3$) is reliably identified with a red galaxy at $z = 0.402$, while source 105A is 10″ north of a quasar at $z = 1.10$. Because source 105A has very low surface brightness, and the optical identification is offset along the radio major axis (see contour map of WHK), the quasar could be the correct identification of 49/W3.

6. For 21 cm source 31 (not detected at 6 cm), a reliable optical identification has now been found, which was not recognized before on the basis of the less accurate WSRT 21 cm position (WKK). The same radio source in the deeper WSRT map of OW is in fact close to a blue galaxy, whose magnitudes were derived from unpublished photometry by KKW. With respect to the VLA 21 cm position, the blue galaxy is at $\Delta R.A.(VLA - opt) = -1″.8$ and $\Delta decl.(VLA - opt) = -0″.5$.

In summary, our best guess is that radio sources 7/W2, 9/W1, 46/W3, and 21 cm source 31 are correctly identified and that the proposed identifications of 49/W3 and 21 cm source 36 are less likely to be correct. Among the 6 doubtful identifications above, one is a Galactic star, one is a quasar, one is a red galaxy, and three are blue galaxies, roughly in proportion with the identification fractions to be discussed in § V. All other identifications given for the complete radio optical sample in Table 2 are considered to be correct on the basis of their very good radio-optical positional coincidence ($LR \gg 2.0$).

We expect that a larger fraction of the claimed blue radio galaxy identifications will be due to contamination (as KKW predicted), because of the higher surface density of blue field galaxies. In our sample, however, most of the candidate blue galaxy identifications actually have a very high likelihood ratio ($LR \geq 8$), as high as those of the red galaxies. We therefore believe that most of the blue radio galaxy identifications are correct. This is further supported by recent VLA 21 cm mapping of the LBDS radio sources with the VLA A array (Oort et al. 1987). They found that most of the claimed blue radio galaxy identifications are correct, although the fraction of misidentifications among the claimed blue galaxies (5 out of 30, or 17%) is indeed higher than that for the red galaxies (1 out of 34, or 3%). The VLA A array positions thus indicate an overall reliability for the LBDS identification sample of 91% (58/64), very close to the values claimed by WKK and in this paper. In addition, the high-resolution maps of Oort et al. (1987) show that the red galaxies are almost exclusively extended or resolved radio sources at the 1″ resolution of the VLA, while the proposed blue galaxy identifications are generally compact radio sources, unresolved even at 1″ resolution. The distinction between the red and the blue radio galaxy population thus corresponds to a clear distinction in radio source morphology. The fact that the smaller, unresolved sources naturally have smaller position errors makes it very unlikely that most blue galaxies are misidentifications. From all this evidence we conclude that the claim of Wall et al. (1986), that the blue sub-mJy radio galaxies are largely misidentifications or misclassifications, cannot be correct.

c) The Photometry and Spectroscopy

The photometry was derived from WMOKK and its quality is described in detail by KKW. Reproductions of the four-band PDS images used for the photometry are given by WMOKK. The standard aperture for most objects was 7″.5 in diameter. The J magnitude zero points were derived from an available photoelectric sequence. The color zero points were derived from the bimodal color distribution of faint stars with an accuracy of about 0.15 mag in each color. (No correction for Galactic absorption was made, because the method for determining the color zero points already takes out most of the reddening; see KKW).

Spectroscopic redshifts have been determined thus far for 16 sub-mJy radio sources in the 21 cm VLA sample as a part of the long-term project of KKW on the Kitt Peak 4 m Cryogenic Camera to measure the redshift distribution of faint radio galaxies, quasars, and field galaxies. An update of the published redshifts of KKW is given in the fourteenth column of Table 2. A complete description of the spectroscopic data, as well as their analysis, will be given by Koo, Kron, and Windhorst (1987).

The $UJFN$ magnitudes for our sample sources are listed in the tenth through thirteenth columns of Table 2 and their redshifts in the fourteenth column.

d) Constraints from Optical Identifications and Photometry

We have complete optical identification information only for the radio source sample selected at 21 cm. The portions of the complete 21 cm VLA sample that lie within our 6 cm VLA fields contain 54 radio sources with $S_p > 5.0$ and attenuation factor < 10.0. Among these, 27 have proposed identifications with $LR > 2.0$. Two *spurious* objects are expected (see the discussion of WKK), presumably among the objects with $LR \approx 2.0$ discussed in § IIIb. Only one *real* identification is expected to be missing (with $LR < 2.0$). Hence, the total expected identification fraction, corrected for the expected contamination and incompleteness, is 26/54 (48% $\pm$ 9%). The sample reliability is 93% (25 of 27 announced identifications are correct) and its completeness is 96% (25 of 26 expected identifications are indeed announced).

Among the 27 proposed identifications, there are two galactic stars, six quasars, and eight red and 11 blue radio galaxies or presumed galaxies. These proportions are very similar to the identification content of the total 21 cm VLA sample of WMOKK. Hence, selecting the 6 cm fields in regions of higher 21 cm source density has not significantly biased the optical properties of the sample.

The identification fraction of 48% $\pm$ 9% in our sub-mJy VLA sample is consistent with the average 53% of the LBDS sample in the range $1 \lesssim S_{1.46} \lesssim 100$ mJy (WKK), and it is not significantly higher than the 41% $\pm$ 5% identification fraction of the total VLA 21 cm sample (WMOKK).

The fact that the overall identification fraction of radio sources with $S_{1.46} \approx 1$ mJy is as high as $\sim 50\%$ suggests that the underlying population that causes the upturn in the 21 cm counts is already present among the identified sources. The fact that the fraction of identified sources which are blue galaxies increases toward fainter radio fluxes (see § V and also WMOKK and KKW) supports the view that this blue radio galaxy population is most likely responsible for the upturn in the source counts. The fact that the redshifts measured spectroscopically for radio galaxies with $16 \lesssim V \lesssim 22$ mag turn out to be in the range $0.05 < z \lesssim 0.6$, with a median $z_{med} \approx 0.25$ (see also Windhorst, Dressler, and Koo 1986), demonstrates that the sub-mJy radio galaxies are at cosmological distances. Because the identification fraction is $\sim 50\%$ down to $F = 22.7$, the median apparant magnitude in our sample is $F \approx 22.7$ or,

equivalently, $V \approx 23.2$ mag. According to the extensive red-shift data set in the updated Hubble diagram of KKW, supplemented by the spectroscopic redshifts in the current sample, these magnitudes imply that the (sub-)mJy sample has a median redshift z_{med} somewhat less than 1, probably around 0.75. Hence the upturn in the source counts is apparently not caused by a local population of very low luminosity dwarf galaxies, as suggested by Wall *et al.* (1986) and Subrahmanya (1986).

IV. THE 6 CENTIMETER SOURCE COUNTS

Now that the complete 6 cm sample has been established, we calculate the source counts at 6 cm. We follow the procedure of PHR to calculate the effective number of sources, N_{eff}, and its error. The solid angle of each of our fields was $\pi(7')^2 = 154$ arcmin^2. The results are given in Table 3. We choose the upper limit of the lowest flux density bin to be equal to the threshold for integrated flux density in field W3. Thus

TABLE 3

THE 6 CENTIMETER SOURCE COUNTS IN OUR 462 ARCMIN^2 SURVEY AREA

6 cm Flux Interval (mJy)	Number of Sources	N(eff)	N(exp) Euclidean	N(eff)/N(exp) ($\times 10^{-2}$)
0.10–0.136[a]	1	7.3 ± 7.3	567	1.29
0.136–0.28	5	16.6 ± 8.0	995	1.67
0.28–0.68	10	14.4 ± 4.6	341	4.23
0.60–2.00	13	12.3 ± 4.2	133	10.03
>2.00	1[b]	1.0 ± 1	26	3.85

[a] This bin was normalized to only $\frac{2}{3}$ the area of the others, because it was below the completeness level of Wind 3.

[b] We expect low counts in this bin because of the way the survey area was selected; see § IV.

only two fields contribute to the source counts in the lowest bin, and the expected source density is calculated accordingly.

Following the procedure of earlier observers (see, e.g., Fomalont *et al.* 1984; PHR), we normalize our source counts to the differential source count expected in a static, homogeneous, Euclidean world model:

$$dN = 90S^{-2.5}dS \ sr^{-1} .$$

Two remarks about the results in Table 3 are in order. First, the Lynx.2 area surveyed by WMOKK had only a few 21 cm sources brighter than ~ 3 mJy. Hence the lack of sources brighter than a few mJy in our survey at 6 cm is not surprising.

Second, as mentioned in § Ia, the 6 cm field centers were selected to cover the maximum number of known 21 cm sources. This introduces a small bias in the overall source counts, which we estimate here. The total area covered by our three 6 cm fields within their 7' radii is $3\pi(7')^2$ or 462 arcmin^2. The boundaries of our fields extended to 20' from the center of the 21 cm map. Our three fields covered 37% of the area within 20' of the 21 cm map center. Of the 85 sources of the complete 21 cm catalog of WMOKK lying inside the 20' circle, 48 also lay in one of our 6 cm fields (six 6 cm sources coincident with cataloged 21 cm sources lay just outside the 7' boundaries of our fields). Hence, the 6 cm catalog survey area included 56% of the sources in the 21 cm sources, while covering only 37% of the area. As a consequence, the particular selection of the 6 cm fields could result in source counts that are high by a factor $56/37 = 1.51$ at most.

Our results are compared with previous work in Figure 1, adopted from PHR. Our 6 cm counts in the Lynx.2 area are perhaps $\sim 30\%$ higher than those in the other areas, although the differences are not significant given the limited statistics in all surveys. The overall slope of the source counts in Lynx.2
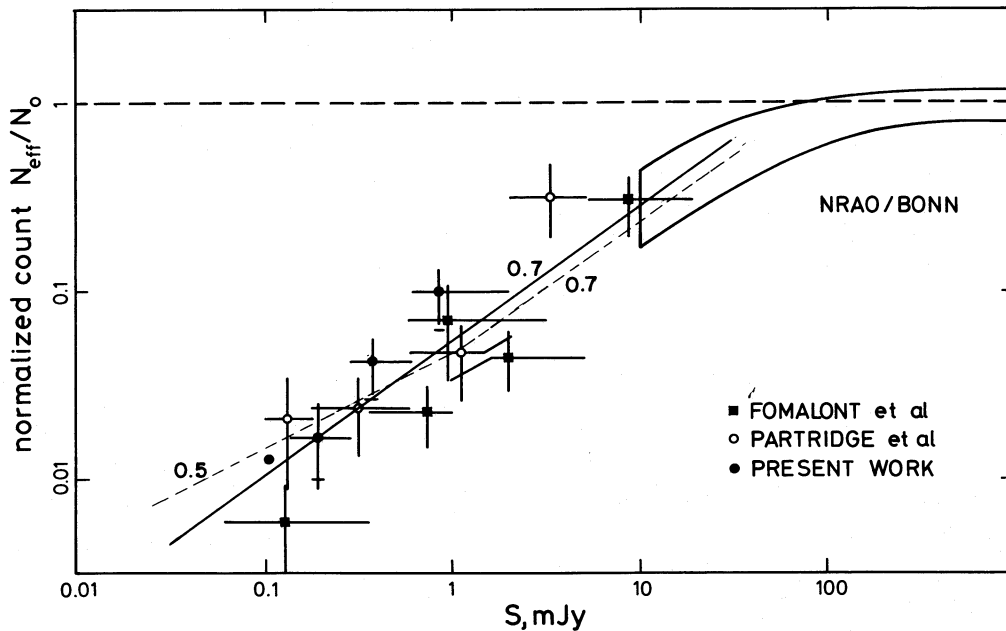
FIG. 1.—The normalized differential 6 cm source counts. Filled circles are our 6 cm counts in Lynx.2. Light ticks mark the limit of the possible overestimation of the source counts discussed in § IV. Open circles are the 6 cm counts in the areas of PHR, and filled squares are the 6 cm counts of Fomalont *et al.* (1984). The counts from brighter surveys are taken from Fomalont *et al.* and PHR. One sigma error bars are given for the fainter surveys. Our faintest point is drawn without error bars, because it was only based on one source. Solid line of slope ~ 0.7 (corresponding to $dN \propto S^{-1.8}$) is the best fit to all points with $S_{4.86} \lesssim 30$ mJy. Dashed line segments of slope ~ 0.7 (for $2 \lesssim S_{4.86} \lesssim 30$ mJy) and ~ 0.5 (for $0.1 \lesssim S_{4.86} \lesssim 1$ mJy) indicate the possible change in slope of the 6 cm source counts that would be consistent with the upturn in the 21 cm counts.

agrees well with that of the other 6 cm VLA surveys (Fomalont *et al.* 1984; PHR).

We have estimated the slope of the best-fit line through the data points of Figure 1 for $S \lesssim 10$ mJy. It is 0.7 ± 0.1, corresponding to $\gamma \approx 1.8$ if $(dN/dS) \propto S^{-\gamma}$. This value is consistent with the slope of the 6 cm source counts reported by PHR. We also investigated whether the observed change of slope in the 21 cm source counts is consistent with the current 6 cm counts, by fitting lines to two flux density regimes, $2 \lesssim S_{4.86} \lesssim 30$ mJy and $0.1 \lesssim S_{4.86} \lesssim 1$ mJy (*dashed lines* in Fig. 1). The data are consistent with a change of slope of ~ 0.2 at $S_{4.86} \sim 1$–2 mJy, with $\gamma \approx 2.0$ for $S_{4.86} \lesssim 1$ mJy, especially if we exclude the lowest point of Fomalont *et al.* (1984) from the fit. Thus our 6 cm source counts are consistent with the gradual change in slope of the normalized differential counts at 21 cm reported by WMOKK and discussed in § I here, although such a change in slope cannot be noticed in the 6 cm counts alone. This is partly due to the poorer statistics at 6 cm, but it may also suggest that the sources contributing to the upturn of 21 cm counts do not in general have flat spectra. This point is discussed further in the next section.

V. THE SPECTRAL INDEX DISTRIBUTIONS

a) Spectral Indices and Their Errors

One of the aims of this work is to obtain spectral indices for sub-millijansky sources. The spectral indices were calculated from our integrated 6 cm flux densities and the 21 cm fluxes from WMOKK by using:

$$\alpha = -(\log S_1 - \log S_2)/(\log v_1 - \log v_2)$$

with $v_1 = 1462$ MHz and $v_2 = 4860$ MHz. The beam size and flux determining algorithms at 21 and 6 cm are similar, so that no surface brightness dependent biases are expected to affect the values of α substantially. The error in each calculated value of spectral index was found by taking the quadrature sum of the errors in the two flux densities, S_1 and S_2:

$$\sigma_\alpha = \{\sqrt{[(\sigma_{S_1}/S_1)^2 + (\sigma_{S_2}/S_2)^2]}\}/(\ln v_2 - \ln v_1) .$$

As noted in § II*h*, some of the sources in the 21 cm sample that lay within our 7′ fields were not detected in our 6 cm survey at the 4 σ level. For these sources, we inspected our maps to see if they showed up at the $3 \sigma < S_p < 4 \sigma$ level. If so, we entered their 6 cm flux in Table 2 (with an asterisk), and otherwise we established a *lower* limit on the spectral index by assuming that the 6 cm density was at or below the $\sim 3 \sigma$ threshold level. Likewise, we convincingly detected some new sources at 6 cm that were not found previously at 21 cm. In these cases, *upper* limites on the spectral index α were determined by assuming that the 21 cm map flux density was $\leq 3 \sigma = 135 \mu$Jy. In two cases, a reexamination of the original 21 cm maps down to the 3σ level allowed us to make an actual determination of the 21 cm flux, improving our estimates of the spectral indices. These sources are marked in Table 2 by an asterisk behind the 21 cm flux in the fifth column.

The spectral indices determined between 21 and 6 cm are listed in the seventh column of Table 2. Our calculation of the spectral indices assumes that the radio sources have not varied in the 4 yr interval between the 21 cm observations (epoch 1982.0) and the 6 cm observations (epoch 1986.1) reported here. The work of OW and WMOKK demonstrated that significant variability occurs in about 5% of the mJy and sub-mJy radio source population. (In our complete 21 cm sample of 54

sources, only sources 14/W1, 22/W1, and 47/W3 were found to vary significantly on time scales of 1 month to 1 yr. Source 18/W2 is also variable, but does not belong to the complete 21 cm sample). Hence, the statistical studies of the spectral index distribution discussed below will not be biased seriously by source variability on time scales of 1 month to 1 yr. However, we cannot rule out some variability on longer timescales for a minority of the sub-mJy population, *nor* variability at 6 cm of sources which do not vary much at 21 cm. Either would appear as a broadening of the spectral index distribution.

In the eighth column of Table 2 we give a one character classification of the spectral indices: F = flat spectrum ($0 \leq \alpha < 0.5$); S = steep spectrum ($\alpha \geq 0.5$); and I = inverted spectrum ($\alpha < 0$). In most cases, assignment to one or another of these categories is unambiguous. In some cases (such as source 36/W1 with $\alpha = 0.53 \pm 0.29$), the error bars are large enough to include values of $\alpha > 0.5$ or $\alpha < 0.5$ and hence to make assignment to a spectral index category uncertain. Since there are more sources with $\alpha > 0.5$ than with $\alpha < 0.5$, errors in the spectral classification might tend to increase the claimed fraction of flat spectrum sources.

b) Possible Biases in the Spectral Index Distribution

In the remainder of this section we will study the dependence of the spectral index distribution $N(\alpha)$ on flux density. We consider the following parameters of the spectral index distribution in each flux density interval: the fraction of flat and inverted spectrum sources $f(\alpha < 0.5)$; the median spectral index α_{med}; the mean of the spectral index distribution $\langle \alpha \rangle$ (assuming that the actual spectral index for objects with only an upper limit to α is equal to that value minus the value of σ_α and that the actual spectral index for objects with only a lower limit is that value plus σ_α); and the dispersion in the mean, $\sigma_{\langle \alpha \rangle}$, assuming a Gaussian shape for the spectral index distribution.

There are four selection effects on the spectral index distribution that we must take care of properly first:

1. The error in the spectral indices increases for weaker sources due to their lower signal-to-noise ratio. This will result in a broadening of the spectral index distribution for the weaker sources. If one cuts the samples off at sufficiently high signal-to-noise ratio (≥ 7) this broadening will no longer be the dominant factor (compare Fig. 2*a* with 2*b*, or 3*a* with 3*b*).

2. We must include in our analysis both the measured values and the upper and lower limits to α given in the seventh column of Table 2. Our 6 and 21 cm surveys were made to comparable depth for sources with spectral indices around the median of the sample ($\alpha_{med} \approx 0.7$; the 5 σ flux limits are ~ 75–100 and 225 μJy, respectively), so that the number of upper or lower limits should not be too large. This number would be prohibitive—and the resulting statistics derived from the spectral index distributions meaningless—if the surveys at the two different frequencies were not of comparable depth, or if the upper limits to source fluxes at one frequency were not set stringently enough. For that reason, we searched in our 21 or 6 cm maps down to the 3 σ level, if a source was convincingly detected at the other wavelength.

3. In addition, there will be a bias against steep spectrum sources if we consider the faintest sources in a sample selected at 21 cm, and a bias against flat spectrum sources if we consider the faintest sources in a sample selected at 6 cm, because of the sample selection threshold at the other wavelength. This bias is discussed in more detail by Katgert (1976) and Wind-
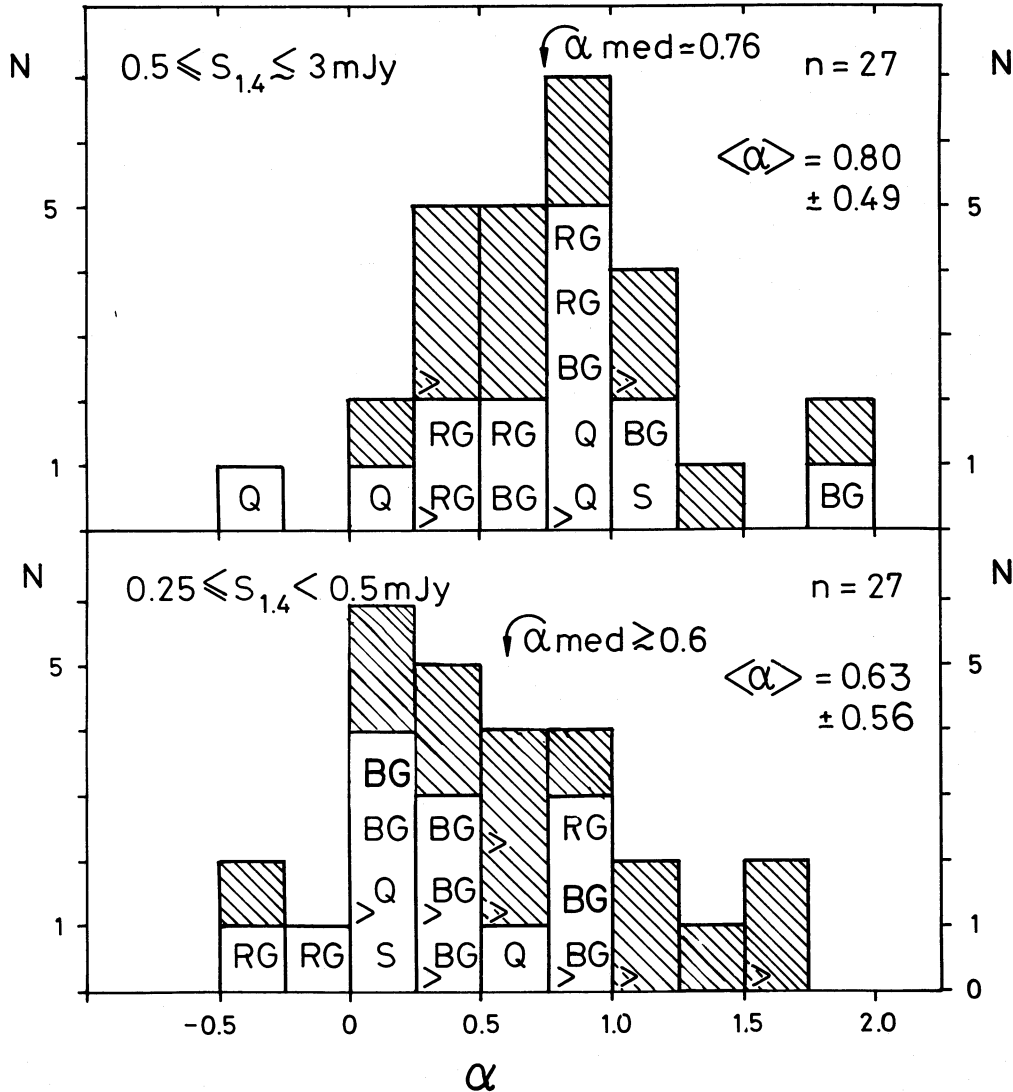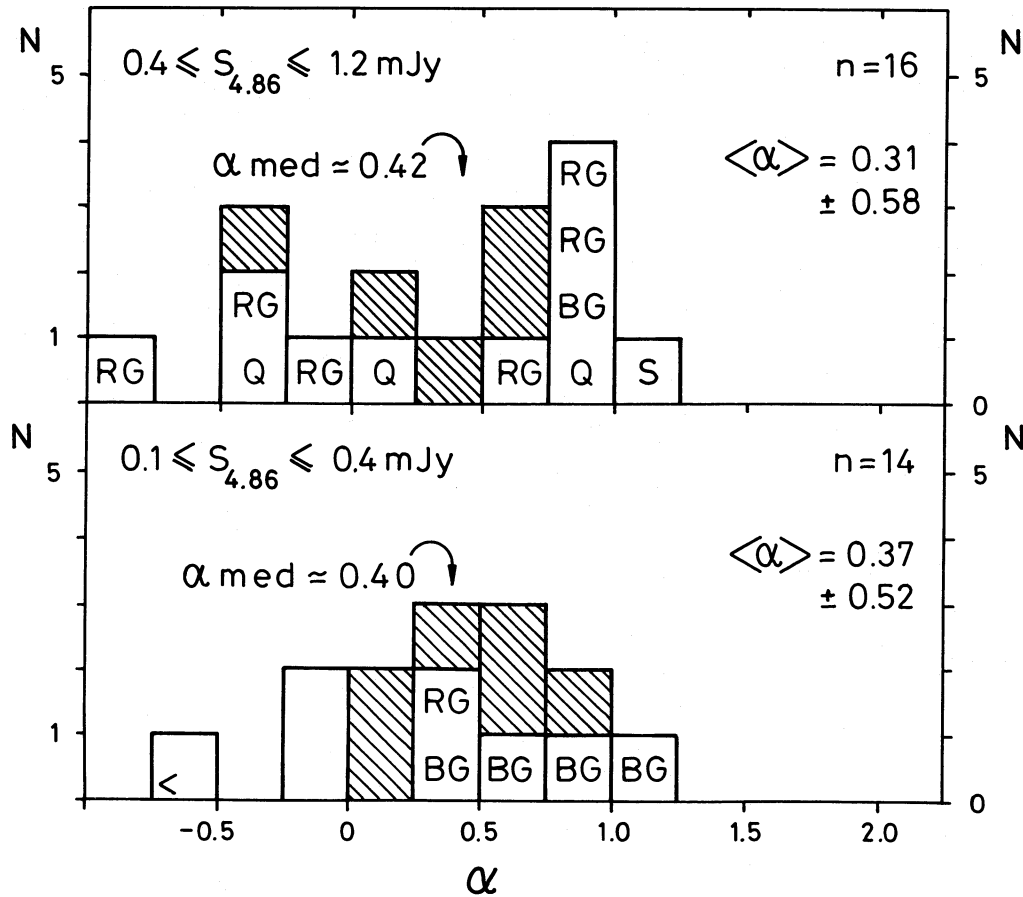
FIG. 2.—The spectral index distribution for all radio sources in the complete 21 cm sample in the flux density ranges $0.50 \leq S_{1.46} \lesssim 3$ mJy (Fig. 2a) and $0.25 \leq S_{1.46} < 0.50$ mJy (Fig. 2b). The optical identifications are indicated as follows: RG = red galaxy, BG = blue galaxy, Q = quasar, S = Galactic star. Shaded areas denote the unidentified radio sources; the > symbol indicates a lower limit on α.

horst and Oppe (1987) and is most easily corrected for by cutting the sample off appropriately in flux density (see under point [4], below).

4. As noted in § IId (see also WHK and PHR), faint sources are underrepresented in our sample because of the primary beam response of the individual telescopes; the faintest sources are detected only near the center of the primary beam. If the sample is selected at one frequency, this is not a serious bias if the spectral index distribution does not change with flux density (which is to first order indeed the case, as we will see below). However, the bias induced by the primary beam effect is potentially more serious if sample selection thresholds at two different frequencies are involved and if the areas covered by the primary beams at the two different frequencies are not the same, as in our case.

The combined effect of bias (3) and (4) is that the sample becomes gradually less complete in α at fainter fluxes. Again, the remedy is to cut the sample off more severely in sky flux, as demonstrated by W84 and Windhorst and Oppe (1987), and to

give a careful discussion of the selection effects whenever they are relevant at the faintest fluxes. Because essentially all our 6 cm sources are within the -3.5 dB attenuation contour of the 21 cm map, bias (3) and (4) can be effectively cured by taking a $\sim 10\,\sigma$ instead of a $5\,\sigma$ cutoff in the 21 cm sample. In that case, the true number of weak 6 cm sources can be estimated by taking the values of $N_{\rm eff}$ as computed in § IV, rather than the direct source counts. The effect is to increase value of f marginally. This suggests that the fainter sources in each flux density category—those with the largest values of $N_{\rm eff}$—usually have flatter spectra, consistent with the trend in the spectral index distribution that we will discuss below.

c) Spectral Index Distribution versus 21 Centimeter Flux Density

We first study the dependence of the spectral index distribution $N(\alpha)$ on 21 cm flux density, because we have complete optical identification information for the sample selected at 21 cm. In Table 4 and Figure 2 the spectral index distributions

FIG. 3.—The spectral index distribution for all radio sources in the complete 6 cm sample in the flux density ranges $0.4 \leq S_{4.86} \lesssim 1.2$ mJy (Fig. 3a) and $0.10 \leq S_{4.86} < 0.40$ mJy (Fig. 3b). The optical identifications are indicated as in Fig. 2; the < symbol indicates an upper limit on α.

are given for two different 21 cm flux intervals, as well as the optical identification percentages of the relevant classes of radio sources. The lower boundary of the lowest flux interval is chosen at a sky flux of $S_{1.46} = 0.25$ mJy ($\sim 9\ \sigma$ in the natural weighted map of WMOKK) to minimize the biases discussed above. The upper boundary of the highest flux interval is chosen to be a factor of 12 above the lower boundary of the lowest flux interval. This excludes the brightest sources, which—because of the selection of the fields—do not form a complete sample. The two flux intervals are chosen so as to contain roughly equal number of sources. The fraction of very steep spectrum sources will be underestimated for the weakest sources, because sources near the 0.25 mJy threshold of our 21 cm sample will appear in the 6 cm sample only if $S_{4.86} \gtrsim 0.06\ \mu$Jy (3 σ), that is if $\alpha \lesssim 1.2$. Figure 2 shows that indeed the faintest flux density bin has proportionally fewer values of $\alpha \gtrsim$

1. For $S_{1.46} \gtrsim 0.50$ mJy this bias is less important, and only a few upper limits are seen.

The median spectral index for radio sources with $S_{1.46} > 0.5$ mJy is $\alpha_{med} \approx 0.76$ (the two lower limits below this value do not affect this very much). For radio sources with $0.25 \lesssim S_{1.46} < 0.5$ mJy we find $\alpha_{med} \gtrsim 0.6$, a value that is underestimated because of the larger fraction of lower limits to α in the faintest flux density bin. Hence, the true median is larger, possibly as large as for the brighter sample. The mean spectral index and its Gaussian dispersion are 0.80 ± 0.49 for the brighter interval and 0.63 ± 0.56 for the fainter interval, the latter value again probably somewhat underestimated because of the larger fraction of lower limits on α. The errors in these numbers are a combination of intrinsic spread in the distribution and measurement errors. The fraction of flat spectrum sources, $f(\alpha < 0.5)$, is 22% $\pm$ 7% for the brighter sample and

TABLE 4

THE SPECTRAL INDEX DISTRIBUTION VERSUS 21 CENTIMETER FLUX DENSITY

1462 MHz FLUX INTERVAL (mJy)	MEDIAN α	MEAN $\pm$ σ	$f(<0.5)$	OPTICAL IDENTIFICATION CLASSES					
				Galactic Stars	Quasars	Blue Galaxies	Red Galaxies	Total Identifications	Unidentified
$0.50 < S < 3.00$........	0.76	0.80 0.49	6/27 (22%)	1/14 (7%)	4/14 29%)	4/14 (29%)	5/14 (35%)	14/27 (52%)	13/27 (48%)
$0.25 < S < 0.50$........	>0.60	0.63 0.56	11/27 (41%)	1/13 (8%)	2/13 (15%)	7/13 (54%)	3/13 (23%)	13/27 (48%)	14/27 (52%)

40% ± 10% for the fainter sample. (Since objects with lower limits were considered together with their formal errors, only one out of the three lower limits that occur with $\alpha < 0.5$ is expected actually to have $\alpha > 0.5$, so that $f(\alpha < 0.5)$ is not significantly affected by including these lower limits. Again, the apparently higher fraction $f(\alpha < 0.5)$ in the fainter flux bin is at least partially due to the larger fraction of steep spectrum sources missed.

In summary, to first order the spectral index distribution for the complete 21 cm sample does not change very much with 21 cm flux below 1 mJy. Its mean and median stay around $\alpha_{med} \approx 0.75$, with a Gaussian dispersion of about 0.5. The apparent larger fraction of flat spectrum sources at fainter fluxes is at least in part due to the stronger selection against steep spectrum sources (see § Vb). It seems safe to conclude that the majority of the sub-mJy radio source population *selected at 21 cm* is of the steep spectrum class.

d) Spectral Index Distribution versus 6 Centimeter Flux Density

In this section we study the dependence of the spectral index distribution $N(\alpha)$ on *6 cm* flux density. In Table 5 and Figure 3 the spectral index distributions are given for two different 6 cm flux intervals, as well as the optical identification percentages of the relevant classes of radio sources. (Note that optical identification information is not available for the three sources with the flattest radio spectra in the lowest flux density bin.)

The lower boundary of the lowest flux interval is chosen at a sky flux of $S_{4.86} = 0.10$ mJy ($\sim 7 \sigma$) to reduce the biases discussed in § Vb. The two flux intervals were again chosen so as to contain roughly equal number of sources. The fraction of inverted spectrum sources will be underestimated for the weakest sources, because sources near the 0.10 mJy threshold, of our 6 cm sample will appear in the 21 cm sample only if $S_{1.46} \gtrsim 0.086 \mu$Jy (3 σ), that is if $\alpha \gtrsim -0.1$. Figure 3 shows that the faintest flux density bin has perhaps somewhat fewer objects for $\alpha \lesssim -0.1$. For the brighter flux bin ($S_{4.86} \gtrsim 0.40$ mJy) this bias is unimportant.

The median spectral index for radio sources with $S_{4.86} > 0.4$ mJy is $\alpha_{med} \approx 0.42$. For radio sources with $0.10 \lesssim S_{4.86} < 0.4$ mJy we find $\alpha_{med} \gtrsim 0.40$, a value that may be somewhat overestimated because of the sources with inverted spectra that have been missed in the faintest flux density bin. The mean spectral index and its Gaussian dispersion are 0.31 ± 0.58 for the brighter flux interval and 0.37 ± 0.52 for the fainter interval. Hence, to first order the spectral index distribution for the complete 6 cm sample does not change very much with 6 cm flux below 1 mJy. Its mean and median stay around $\alpha_{med} \approx 0.4$, with a Gaussian dispersion of about 0.5.

The fraction of flat spectrum sources, $f(\alpha < 0.5)$, is

50% ± 5% for the brighter 6 cm sample and about 57% ± 10% for the fainter sample. The latter number is of course a lower limit, because of the larger fraction of flat and inverted spectrum sources missed in the lowest density bin. Because we do not know the true spectral index distribution in the lowest flux density bin, we cannot correct the value of $f(\alpha < 0.5)$ for the selection against the flat and inverted spectrum sources. However, our data seems to be consistent with a somewhat larger fraction of flat spectrum sources at fainter flux levels in samples selected at 6 cm.

The fraction of flat and inverted spectrum sources in both the brighter and the fainter samples selected at 6 cm is of course higher than the corresponding fractions for the samples selected at 21 cm. This is merely the consequence of the different selection frequencies. The higher selection frequency will tend to pick up a higher fraction of flat spectrum sources at any flux level.

In conclusion, the sub-mJy radio source population selected at 6 cm is more a mixture of steep spectrum sources on the one hand and flat and inverted spectrum sources on the other than the sample selected at 21 cm. The median of the spectral index distribution is about 0.4 and does not change drastically with flux density. However, keeping the selections against flat and inverted spectrum sources at the faintest flux level in mind, the distributions are consistent with the existence of a somewhat larger fraction of flat spectrum sources at fainter fluxes in the sample *selected at 6 cm.*

e) Spectral Index Distribution versus Optical Identification Class

Let us now consider the optical identification content as a function of spectral index and flux density. Tables 4 and 5, as well as Figures 2 and 3, show a few noteworthy features:

1. The fraction of blue galaxy identifications increases significantly toward fainter fluxes. While in the brighter flux density sample the fraction of red galaxies is larger than the fraction of blue galaxies, especially in the sample defined at 6 cm, in the fainter flux density sample the blue galaxy population is the dominant population by at least a factor of 2:1. As noted in § IIIb, this effect is real and not merely due to a larger amount of misidentification and contamination at fainter fluxes. This result is consistent with the conclusion of KKW that the blue radio galaxy population begins to dominate at levels below $S_{1.46} \lesssim 5$ mJy and of WMOKK that it is the most likely candidate to cause the upturn in the source 21 cm counts below a few mJy.

2. The blue radio galaxies in general have steep spectral indices with $\alpha_{med} \approx 0.75$. This precludes the possibility that most of the radio emission is of thermal origin. These steep

TABLE 5

THE SPECTRAL INDEX DISTRIBUTION VERSUS 6 CENTIMETER FLUX DENSITY

4860 MHz FLUX INTERVAL (mJy)	MEDIAN α	MEAN ± σ	$f(<0.5)$	OPTICAL IDENTIFICATION CLASSES					
				Galactic Stars	Quasars	Blue Galaxies	Red Galaxies	Total Identifications	Unidentified
$0.40 < S < 1.20$........	0.42	0.31	8/16	1/11	3/11	1/11	6/11	11/16	5/16
		0.58	(50%)	(9%)	(27%)	(9%)	(55%)	(69%)	(31%)
$0.10 < S < 0.40$........	0.40	0.37	8/14	0/5	0/5	4/5	1/5	5/11	6/11
		0.52	(57%)	(0%)	(0%)	(80%)	(20%)	(45%)	(55%)

spectral indices are indicative of nonthermal radiation, either due to a nonthermal compact nucleus or to the integrated nonthermal emission arising from the supernovae remnants in a nuclear starburst. We return to these possibilities in § VI.

Three red galaxies in the brighter 6 cm bin—which are the same objects as the red galaxies in the faintest 21 cm flux density bin—have very flat or inverted spectra. One of these, 22/W1 is known to be variable (see § Va), 44/W3 is a bona fide identification and 7/W2 has possibly a doubtful identification (§ IIIb).

3. Remarkably, nine out of 12 (or 75%) of the radio sources in the complete 21 cm sample with $\alpha > 1.0$ are optically *unidentified* (*shaded objects* in Figs. 2 and 3). This is consistent with similar results of KKW, who found that the median (21–50 cm) spectral index of radio sources unidentified on 4 m plates is about 0.85, significantly steeper than the value of 0.70 for the identified radio sources. A similar result was earlier found by Tielens, Miley, and Willis (1979), who showed that the fraction of 4C radio sources identified on Palomar Sky Survey plates is significantly lower for the steepest spectrum category. An explanation for this effect is that the unidentified radio sources are also the most distant ones, so that the *K*-correction steepens the radio spectra. (The radio spectra are assumed to be intrinsically much steeper at higher rest-frequencies due to the higher synchrotron losses; see § VIb.)

f) Three-Point Spectral Indices

Some of the brighter sources in the 6 cm sample also have 50 cm flux densities measured with the WSRT by Windhorst and Oppe (1987); see also W84. This allows us to study three point spectral indices for a complete subsample of mJy radio sources. The 50 cm map of the Lynx.2 area (epoch 1982.0) had an rms noise of 0.42 mJy, and we inspected the map down to its 3 σ level for sources not given in the list of Windhorst and Oppe. Given the sensitivity of the 50 cm map, we can expect reasonably complete 50 cm information only for those sources in the complete 21 cm sample that have $S_{1.46} \gtrsim 0.90$ mJy. We therefore list in Table 6 all available information at 50, 21, and 6 cm for the complete 21 cm subsample that lies within our 6 cm fields *and* that has $S_{1.46} > 0.90$ mJy. The 21 and 6 cm synthesized beams are very similar, so that the 21–6 cm spectral indices will not be surface brightness dependent. The 50 cm beam, however, is 28″ (HPBW), twice as large as the 21 cm beam. Nevertheless, because the angular size distribution of mJy and sub-mJy radio sources is so narrow ($\theta_{med} \approx$ 3″–5″), we do not expect that the 50–21 cm spectral indices will be seriously overestimated, except for very low surface brightness sources.

Table 6 lists the 50–21 cm spectral index and a low frequency spectral classification analogous to the one from the eighth column of Table 2, as well as the 21–6 cm spectral index and the high-frequency spectral classification and some optical identification information (all from Table 2). In addition, the tenth column of Table 6 gives the spectral curvature SC of the radio source, defined as the low-high frequency spectral index difference, normalized to the combined spectral index error:

$$\text{SC} = [\alpha(50-21) - \alpha(21-6)]/[\sqrt{(\sigma^2_{\alpha(50-21)} + \sigma^2_{\alpha(21-6)})}] .$$

For the few sources that have only upper limits to the measured 50 or 6 cm flux, we assumed in the calculations that their actual low-frequency spectral index is equal to the value of the upper limit $- 1\sigma_\alpha$, and the actual high-frequency spectral index equal to the value of the lower limit $+ 1\sigma_\alpha$, respectively. Source

24 in the 21 sample was not detected at either 50 or at 6 cm, implying an unusual radio spectrum or variability. Because the source coincides with a faint quasar, it may well be variable on time scales of a few years. The other known variable sources in this subsample are the radio star 14/W1 and the very red object 22/W1 (see OW and the discussion in § IIIb). The remaining radio sources we classify in Table 6 as follows: ST for straight spectra, if the absolute value of the spectral curvature is less than one combined sigma; CVX for convex spectra, if SC < −1; and CCV for concave spectra, if SC > +1 (see also Kellerman 1974).

An examination of Table 6 shows that nine radio sources out of the complete subsample of 20 have optical identifications. This 45% identification percentage, as well as the relative identification fractions, are consistent with our findings in § IIId. Most of the identifications in this mJy subsample are red galaxies with straight and steep radio spectra, as can be expected for distant giant elliptical radio galaxies. Half of them also have radio sources that are resolved at the 15″ VLA beam. The one radio source coinciding with a blue galaxy (32/W1) has an extremely concave spectrum. The optical identification is a bright, large and low surface brightness interacting galaxy. The 50 cm beam could thus have seen more flux than the higher frequencies, possibly causing the unusual radio spectrum. The quasars in this subsample have a mix of spectra, one of them possibly affected by variability (21 cm source 24), one having a straight radio spectrum and 49/W3 having a rather concave spectrum. The latter quasar is a low surface brightness radio source, so that its 50 cm radio flux may be larger, as for 32/W1 discussed above.

The most remarkable result from Table 6 concerns the *unidentified* radio sources. Except for the two peculiar concave spectra discussed above (that are possibly a result of a larger beam solid angle at 50 cm), all other significantly concave and convex spectra in Table 6 belong to radio sources *unidentified* on the 4 m plates. And eight out of 11 unidentified radio sources have *concave or convex* spectra, the other three having straight spectra.

In light of the redshift data of KKW, it is most likely that red radio galaxies not visible on the 4 m plates ($F > 22.7$) have $z \gtrsim 0.9$, while the blue radio galaxies beyond the 4 m plate limits have redshifts at least > 0.5 and possibly $z \gtrsim 1.0$. Hence we believe that the significantly curved radio spectra of the unidentified source may be due to the radio *K*-correction at high redshifts. We will discuss this possibility in more detail in § VI.

VI. DISCUSSIONS AND CONCLUSIONS

a) Source Counts and Optical Data

In this paper we combined the 6 cm source counts from the Lynx.2 field with those of previous deep VLA 6 cm surveys (Fomalont *et al.* 1984; PHR) and obtained the following picture. The normalized differential 6 cm source counts show strong convergence in the flux density range 0.1–30 mJy, with a slope of $\gamma \approx 1.8[(dN/dS) \propto S^{-\gamma}]$. Below about 1 mJy the slope may flatten somewhat to $\gamma \approx 2.0$, although this cannot be derived from the present 6 cm data alone. The slope of the 6 cm counts at sub-mJy levels, however, is consistent with the gradual change in slope found in the 21 cm counts below $S_{1.46} \lesssim 5$ mJy (W84; WMOKK; Condon and Mitchell 1984).

The amplitude of the normalized differential source counts at the level of a few hundred μJy amounts to 1%–2% of the

TABLE 6

THREE-POINT SPECTRAL INDICES FOR SUB-MILLIJANSKY RADIO SOURCES

Source Number		S608.5 (error) (mJy)	S1462 (error) (mJy)	S4860 (error) (mJy)	α (error) (50/21)	Low-Frequency Spectral Classification	α (error) (21/6)	High-Frequency Spectral Classification	Spectral Curvature		ID	F Mag	z
6 cm/field (1)	21 cm (2)	(3)	(4)	(5)	(6)	(7)	(8)	(9)	Value (10)	Classification (11)	(12)	(13)	(14)
...*	24	<1.89 (0.63)	1.24 (0.11)	<0.48 (0.16)	<0.48 (0.39)	F	>0.78 (0.28)	S	(−2.0)	VAR?	Q	22.99	...
5/W2	32	<1.82 (0.62)	1.65 (0.10)	1.12 (0.13)	<−0.11 (0.39)	F	0.32 (0.11)	F	−1.48	CVX	...	...	...
6/W1	33	4.21 (0.51)	4.64 (0.23)	4.50 (0.10)	−0.11 (0.16)	I	0.03 (0.05)	F	−0.84	ST	Q	21.17	...
11/W2*	40	1.52 (0.41)	0.93 (0.17)	0.60 (0.06)	0.56 (0.37)	S	0.36 (0.17)	F	+0.49	ST	...	...	...
14/W1	44	4.05 (0.69)	1.91 (0.12)	0.54 (0.02)	0.86 (0.21)	S	1.05 (0.06)	S	−0.87	VAR	S	15.64	0.000
19/W1	48	8.08 (0.82)	2.71 (0.20)	1.15 (0.04)	1.25 (0.14)	S	0.71 (0.07)	S	+3.45	CCV	R?	>22.7	(>1.0)
22/W1	52	2.98 (1.07)	1.35 (0.12)	0.72 (0.03)	0.90 (0.42)	S	0.52 (0.08)	S	+0.89	VAR	...	...	...
24/W1	53	2.38 (0.54)	0.74 (0.10)	0.31 (0.04)	1.33 (0.30)	S	0.72 (0.15)	S	+1.82	CCV	...	...	...
26/W2*	55A	8.85 (0.70)	2.36 (0.14)	0.26 (0.07)	1.51 (0.11)	S	1.84 (0.22)	S	−1.34	CVX	...	...	...
30/W2	61	2.96 (0.63)	0.92 (0.06)	0.37 (0.02)	1.33 (0.25)	S	0.76 (0.07)	S	+2.20	CCV	BG	17.80	0.16
32/W1	63	6.83 (1.20)	1.61 (0.09)	0.64 (0.02)	1.65 (0.21)	S	0.77 (0.05)	S	+4.08	CCV	...	...	...
35/W1	65	2.47 (0.52)	1.75 (0.10)	0.74 (0.04)	0.39 (0.25)	F	0.72 (0.06)	S	−1.28	CVX	...	...	...
39/W2	69B	<1.52 (0.51)	1.06 (0.09)	0.79 (0.05)	<−0.41 (0.39)	F	0.24 (0.09)	F	−0.55	ST	...	...	...
43/W2*	72	7.68 (0.61)	2.85 (0.16)	0.75 (0.11)	1.13 (0.11)	S	1.11 (0.13)	S	+0.12	ST	...	...	...
...*	94	3.14 (0.41)	1.93 (0.13)	<0.49 (0.16)	0.56 (0.17)	S	>1.14 (0.28)	S	−2.63	CVX	RG?	22.08	(0.8)
...*	104	1.61 (0.38)	0.95 (0.08)	<0.54 (0.18)	0.60 (0.29)	S	>0.46 (0.28)	F	−0.35	ST	Q	21.36	1.10
49/W3	105A	6.92 (1.29)	1.96 (0.24)	0.67 (0.09)	1.44 (0.25)	S	0.89 (0.15)	S	+1.89	CCV	RG	20.05	0.402
50/W3	105B	4.37 (0.79)	1.79 (0.17)	0.68 (0.05)	1.02 (0.23)	S	0.81 (0.10)	S	+0.84	ST	RG	21.96	0.76
54/W3	108	5.08 (0.53)	2.31 (0.17)	0.73 (0.04)	0.90 (0.15)	S	0.96 (0.08)	S	−0.35	ST	...	...	...
58/W3*	113	4.57 (0.46)	2.85 (0.26)	0.59 (0.30)	0.54 (0.16)	S	1.31 (0.42)	S	−1.71	CVX	...	...	...

Col. (1).—6 cm source number and 6 cm field where the source was found. (Asterisk = source not in complete 6 cm sample).
Col. (2).—21 cm source number. (Asterisk = source not in complete 21 cm sample).
Col. (3).—50 cm (608.5 MHz) total sky flux and its error, or 3 σ upper limit.
Col. (4).—21 cm (1462 MHz) total sky flux and its error, or 3 σ upper limit.
Col. (5).—6 cm (4860 MHz) total sky flux and its error, or 3 σ upper limit.
Col. (6).—50–21 cm spectral index and its error. If source not detected at 50 cm, then a lower limit is given.
Col. (7).—S = steep ($\alpha > 0.5$), F = flat ($0 < \alpha < 0.5$), I = inverted ($\alpha < 0$).
Col. (8).—21–6 cm spectral index and its error. If source not detected at 6 cm, then an upper limit is given.
Col. (9).—S = steep ($\alpha > 0.5$), F = flat ($0 < \alpha < 0.5$), I = inverted ($\alpha < 0$).
Col. (10).—Spectral curvature SC:[(50–21 cm spectral index) − (21–6 cm spectral index)]/(combined spectral index error).
Col. (11).—Spectral curvature classification: ST = straight spectrum ($-1 < SC < 1$), CVX = convex spectrum ($SC < -1$), CCV = concave spectrum ($SC > +1$), VAR = variable radio source.
Col. (12).—Optical candidate: RG = red galaxy (gE), BG = blue galaxy (gE), G? = probable galaxy, Q = quasar, S = Galactic star, ... = unidentified.
Col. (13).—Photographic F magnitude.
Col. (14).—Spectroscopic redshift (if not measured, then within parenthesis z-estimate from magnitude and colors after KKW).

maximum in the differential counts at *both* frequencies. The change in slope in the normalized differential counts is ~ 0.3 at 21 cm and could be ~ 0.2 at 6 cm. It is more easily visible at 21 cm, because the 21 cm statistics are better (the primary beam covers $\sim 10 \times$ more solid angle than at 6 cm). The change in slope at 21 cm occurs at $S_{1.46} \sim 5$ mJy according to WMOKK, while Figure 1 (and PHR) suggest it would occur around $S_{4.86} \approx 1$–2 mJy at 6 cm. This is consistent with the fact that the majority of the radio source population around a few mJy is of the steep spectrum class.

The nature of the radio source population(s) that causes this apparent upturn has been the cause of much discussion in the recent literature (see e.g., W84; WMOKK; Condon 1984; Wall *et al.* 1986; Subrahmanya 1986). This debate has been reviewed to some extent in our introduction. Here we will confine ourself to a summary of the available optical and radio data which may help to constrain the nature of the radio sources that dominate the faint source counts.

For the subsample of 21 cm sources within our 6 cm fields, the total optical identification fraction, corrected for the expected contamination and incompleteness, is 26/54 (48%), with a sample reliability of 93% and completeness of 97%. Our identification fraction is not significantly different from that at the mJy level in the WSRT samples of WKK or the sub-mJy sample of WMOKK. The fact that the overall identification fraction of radio sources with $S_{1.46} \approx 1$ mJy is as high as $\sim 50\%$ suggests that the underlying population that causes the upturn in the 21 cm counts is already substantially present among the identified sources. More complete optical identifications would provide the best test of this assertion.

The identified fraction of the sub-mJy radio source population consists of a few Galactic stars and about 20% quasars, while the remaining sources are red and blue radio galaxies. The red radio galaxies are morphologically and spectroscopically like giant ellipticals and dominate the radio source identifications at levels brighter than a few mJy (KKW). The blue radio galaxy population consists of some spiral galaxies at brighter magnitudes, but at fainter magnitudes the blue radio galaxies are generally actively starforming (sometimes interacting or merging) galaxies (KKW; WMOKK; Windhorst, Dressler, and Koo 1986). They almost always are compact radio sources, contributing to the very small median angular size of (sub-)mJy radio sources (KKW; OW; Coleman and Condon 1985; Oort *et al.* 1987).

Just as in the 21 cm VLA sample of WMOKK, the fraction of blue radio galaxies in our samples changes from less than one-third at the mJy level to more than two thirds at the sub-mJy level. Hence, just where the change in the slope of the source counts becomes prominent, the blue radio galaxy population becomes increasingly dominant. We therefore reemphasize the conclusion of WMOKK that this blue radio galaxy population is the most likely cause for the upturn in the source counts.

Redshifts have been measured for our radio galaxy sample for $16 \lesssim V \lesssim 22$ mag by KKW. For $V \lesssim 22$ mag the redshifts are in the range $0.05 < z \lesssim 0.6$ with a median $z_{\mathrm{med}} \approx 0.25$, demonstrating that the sub-mJy radio galaxies are at cosmological distances. Because the identification fraction is $\sim 50\%$ down to $F = 22.7$, it was argued in § IIId that the median redshift of the sample is around 0.75. Hence the upturn in the source counts is not caused by a local population of very low luminosity dwarf galaxies, as suggested by Wall *et al.* (1986) and Subrahmanya (1986).

b) Constraints from the Spectral Indices

The characteristics of the spectral index distributions at mJy and sub-mJy levels may be summarized as following. For a complete 21 cm sample with $S_{1.46} \lesssim 3$ mJy the spectral index distribution has a mean and a median of about 0.75, with a Gaussian dispersion of about 0.5, values that do not change very much with flux density. This is consistent with the general trend of the 50–21 cm spectral index distribution in the flux range $3 < S_{1.46} \lesssim 100$ mJy (W84; Windhorst and Oppe 1987). Their data show that the spectral index distribution also has a median of ~ 0.75 over the full range $3 < S_{1.46} \lesssim 100$ mJy. Under the assumption that the radio spectra are to first order straight (for details see § V*e*), we conclude that in the whole range $0.25 \leq S_{1.46} \lesssim 100$ mJy most of the radio sources selected at 21 cm are of the steep spectrum class. The apparently larger fraction of flat spectrum sources in our faintest flux density bin ($0.25 \lesssim S_{1.46} < 0.5$ mJy) is at least in part due to the stronger selection against steep spectrum sources in that bin. However, in view of the relative larger fraction of flat and inverted spectrum sources near the $S_{1.46} = 3$ mJy completeness limit of Windhorst and Oppe (1987), our data is consistent with a somewhat larger fraction of flat and inverted spectrum sources at 21 cm flux levels $\lesssim 0.5$ mJy.

The sub-mJy radio source population selected at 6 cm has a larger fraction of flat and inverted spectrum sources than the one selected at 21 cm, because of the higher selection frequency. The mean and median spectral indices of the complete 6 cm sample are both around 0.4 and do not change drastically with flux density for $S_{4.86} \lesssim 1$ mJy. Allowing for the selection against flat and inverted spectrum sources at the faintest flux level, the distributions are consistent with a somewhat larger fraction of flat spectrum sources at 6 cm fluxes $\lesssim 0.4$ mJy. The results of Table 5 and Figure 3 show that for $S_{4.86} \lesssim 1$ mJy the fraction of flat and inverted spectrum sources, $f(\alpha < 0.5)$, is $\gtrsim 50\%$. This is higher than the $\lesssim 30\%$ flat or inverted spectrum sources found at higher 6 cm flux densities by Condon and Ledden (1981; $S_{4.86} > 15$ mJy) or by Owen, Condon, and Ledden (1983; $S_{4.86} > 35$ mJy). But it is consistent with the data of Fomalont *et al.* (1984) at comparable flux levels, who found that the fraction of flat spectrum sources is $\sim 39\%$ (11/28) down to $S_{4.86} \gtrsim 0.35$ mJy and $\sim 50\%$ (6/12) down to $S_{4.86} \gtrsim 0.07$ mJy. Both their results and ours indicate that at 6 cm the fraction of flat and inverted spectrum sources increases somewhat at the lowest flux densities ($S_{4.86} \lesssim 0.4$ mJy).

It is interesting to note that the spectral indices of the blue radio galaxies in general place them in the steep spectrum class, whether in the sample selected at 6 or at 21 cm. This is consistent with the fact that the bulk of the sub-mJy population have steep radio spectra (§ V) and that the blue galaxies dominate the sub-mJy radio source population (§ III). The steep radio spectra of the blue radio galaxies are consistent with the steep (50–21 cm) spectral index distribution of the blue (and the red) radio galaxy populations at brighter levels (W84; KKW). These papers showed that the median spectral index for $S_{1.46} \gtrsim 1$ mJy is about 0.75, with similar distributions for the red and the blue radio galaxies, except that the fraction of blue radio galaxies with *inverted* spectra is perhaps somewhat larger than that of the red radio galaxies (5 to 1 objects, respectively).

The steep spectral indices of the blue radio galaxies ($\alpha_{\mathrm{med}} \approx 0.75$) preclude the possibility that most of their radio emission at observed $\lambda \gtrsim 6$ cm is of thermal origin. The steep spectral

indices are indicative of nonthermal radiation, due either to a nonthermal compact nucleus or to the integrated nonthermal emission arising from the supernovae remnants in a nuclear starburst (see below).

c) *The Nature of the Sub-millijansky Radio Sources*

We consider here some additional constraints on the nature of the sub-mJy radio sources.

First, we examine the sizes of blue galaxy radio sources. The angular sizes of mJy and sub-mJy radio sources have been studied by OW, Coleman and Condon (1985), and Oort *et al.* (1987). The sub-mJy radio source population has a narrow angular size distribution, consisting of mostly compact radio sources with angular sizes $\lesssim 2''$. The smaller angular scale is already noticeable at the level of a few mJy (OW). The high resolution VLA work of Oort *et al.* (1987) demonstrates that the compact radio sources occur almost exclusively in the blue galaxy population. Their median angular size of $\lesssim 1''$, in combination with their median redshift of ~ 0.2 at $V \approx 20$ mag (§ IIId and KKW), indicates physical sizes for their radio sources of $\lesssim 4$ kpc ($H_0 = 50$, $q_0 = 0.5$). Hence, the radio sources of the blue galaxies are physically quite compact, and the disk as a whole does not contribute most of the radio emission.

The discussion above showed that the sub-mJy blue radio galaxies usually lack significant variability, have mostly steep radio spectra, and are physically quite compact ($\lesssim 4$ kpc). These aspects provide important clues to the nature of the radio emission in the sub-mJy radio galaxies. Here we summarize two possible mechanisms:

1. A nuclear starburst occurring on kpc scales in the galaxy centers. The resulting radio emission would be the consequence of the integrated nonthermal emission of the supernovae associated with the nuclear starburst. This will result in steep radio spectra ($\alpha \sim 0.75$; for a discussion see, e.g., Hummel 1980) and a lack of variability. The prediction in this case is that the radio source will actually be resolved at scales of a few kpc. This could be tested at 6 cm at the VLA in the A array.

2. A nonthermal nucleus on parsec scales. In this case, the sources will be unresolved at the VLA in any of its configurations. The steep radio spectrum ($\alpha \approx 0.75$) would be the consequence of the balance between the injection of fresh synchrotron electrons with their expected initial spectral index of about 0.25 (van der Laan and Perola 1969) and the gradual synchrotron losses, which will steepen the spectral index, starting at the higher frequencies. The observed lack of variability in the mJy population suggests that the radio sources do not in general have recurrent bursts on time scales less than a few years.

The currently available data are consistent with both options. Higher resolution radio observations could decide between them.

Another clue can be obtained from the shape of the radio spectra, keeping the effects of the radio K-correction in mind.

In § Ve we noted the generally steep radio spectra of the *unidentified* radio sources, suggesting the effect of the K-correction at high redshifts. In § Vf we saw that *most* of these unidentified radio sources had *convex or concave* radio spectra.

Let us here explore some possible causes for this phenomenon. From the work of KKW we know that the unidentified mJy radio sources probably consist both of red and blue radio galaxies (at $z \gtrsim 0.75$–1). The red giant elliptical galaxies have, according to Oort *et al.* (1987), almost exclusively extended or resolved radio structures at $1''$ resolution and, according to KKW, usually steep radio spectra. The latter are due to the synchrotron losses in the lobes of their extended radio sources (van der Laan and Perola 1969). Our conjecture is that the unidentified radio sources with convex spectra (and the one object with a straight, steep radio spectrum, 43/W2) are similar giant ellipticals at redshifts $z \gtrsim 1$. The exponential fall-off of the spectrum at the highest frequencies, expected to result from the synchrotron losses in the expanding radio lobes, in combination with the very high redshift, would cause these convex spectra. A prediction of this model is that the unidentified radio sources with convex spectra will be resolved or slightly extended at $\sim 1'$ resolution.

The blue radio galaxies have mostly compact radio sources at $1''$ resolution (Oort *et al.* 1987), and generally steep radio spectra (KKW). One possibility is that these are actively starforming galaxies with a nuclear starburst, in which the physical cause of the starburst (galaxy interaction, merger, gas accretion, etc.) also indirectly triggers nonthermal radio emission from the nucleus. In this model, the nonthermal compact nucleus has a flat spectrum ($\alpha < 0.5$) at high (3–10 GHz) frequencies and is embedded in an extended region of nonthermal emission from the starburst itself, with $\alpha \approx 0.7$. A concave radio spectrum would result. If this model for the blue galaxies is correct, we would expect them to be unresolved at $\sim 1''$ resolution *especially at high frequencies*.

Another possible explanation for the concave spectra of some blue galaxies is that nonthermal ($\alpha \approx 0.7$) radio emission from a nuclear starburst is accompanied by thermal emission ($\alpha \approx 0$) from numerous H II regions associated with the star formation. If this model for the blue galaxies is correct, we would expect their angular size to be comparable at high and low frequencies, and the radio sources might just be resolved at the $\sim 1''$ resolution of the VLA.

REFERENCES

Baars, J. W. M., Genzel, R., Pauliny-Toth, I. I. K., and Witzel, A. 1977, *Astr. Ap.*, **61**, 99.
Coleman, P. H., and Condon, J. J. 1985, *A.J.*, **90**, 1431.
Condon, J. J. 1984, *Ap. J.*, **287**, 461.
Condon, J. J., and Ledden, J. E. 1981, *A.J.*, **86**, 643.
Condon, J. J., and Mitchell, K. J. 1984, *A.J.*, **89**, 610.
Fomalont, E. B., Kellermann, K. I., Wall, J. V., and Weistrop, D. 1984, *Science*, **225**, 23.
Hummel, E. 1980, Ph.D. thesis, University of Groningen.
Katgert, P. 1976, *Astr. Ap.*, **49**, 221.
Kellermann, K. I. 1974, in *Galactic and Extragalactic Radio Astronomy*, ed. G. L. Verschuur and K. I. Kellermann (New York: Springer-Verlag), p.320.

Koo, D. C., Kron, R. G., and Windhorst, R. A. 1987, in preparation.
Kron, R. G., Koo, D. C., and Windhorst, R. A. 1985, *Astr. Ap.*, **146**, 38 (KKW).
Napier, P. J., and Rots, A. H. 1982, VLA Test Memorandum 134.
Oort, M. J. A., Katgert, P., Steeman, F. W. M., and Windhorst, R. A. 1987, *Astr. Ap.*, in press.
Oort, M. J. A., and Windhorst, R. A. 1985, *Astr. Ap.*, **145**, 405 (OW).
Owen, F. N., Condon, J. J., and Ledden, J. E. 1983, *A.J.*, **88**, 1.
Partridge, R. B., Hilldrup, K. C., and Ratner, M. I. 1986, *Ap. J.*, **308**, 46 (PHR).
Subrahmanya, C. R. 1986, talk given at 19th General Assembly of the IAU.
Tielens, A. G. G. M., Miley, G. K., and Willis, A. G. 1979, *Astr. Ap. Suppl.*, **35**, 162.
Thompson, A. R., Clark, B. G., Wade, C. M., and Napier, P. J. 1980, *Ap. J. Suppl.*, **44**, 151.
van der Laan, H., Katgert, P., Windhorst, R. A., and Oort, M. J. A. 1983, in *IAU Symposium 104, The Early Evolution of the Universe and its Present Structure*, ed. G. O. Abell and G. Chincarini (Dordrecht: Reidel), p. 73.

van der Laan, H., and Perola, G. C. 1969, *Astr. Ap.*, **3**, 486.
Wall, J. V., Benn, C. R., Grueff, G., and Vigotti, M. 1986, in *Highlights Astr.*, **7**, 345.
Windhorst, R. A. 1984, Ph.D. thesis, University of Leiden (W84).
Windhorst, R. A., Dressler, A., and Koo, D. C. 1986, in *IAU Symposium 124, Observational Cosmology*, ed. G. Burbidge and L. Z. Fang (Dordrecht: Reidel), in press.
Windhorst, R. A., Kron, R. G., and Koo, D. C. 1984, *Astr. Ap. Suppl.*, **58**, 39 (WKK).
Windhorst, R. A., Miley, G. K., Owen, F. N., Kron, R. G., and Koo, D. C. 1985, *Ap. J.*, **289**, 494 (WMOKK).
Windhorst, R. A., and Oppe, J. 1987, *Astr. Ap. Suppl.*, submitted.
Windhorst, R. A., van Heerde, G. M., and Katgert, P. 1984, *Astr. Ap. Suppl.*, **58**, 1 (WHK).

R. Hank Donnelly and R. Bruce Partridge: Astronomy Department, Haverford College, Haverford, PA   19041-1392

Rogier A. Windhorst: Mount Wilson and Las Campanas Observatories, Carnegie Institution of Washington, 813 Santa Barbara Street, Pasadena, CA   91101